

**REPUBLIC OF TURKEY
YILDIZ TECHNICAL UNIVERSITY
GRADUATE SCHOOL OF NATURAL AND APPLIED SCIENCES**

**FINITE ELEMENT ANALYSIS OF STRUCTURAL PROBLEMS
WITH FUNCTIONALLY GRADED MATERIALS
USING HIGHER ORDER ELEMENTS**



HANAN ALIMAM

**MSc. THESIS
DEPARTMENT OF CIVIL ENGINEERING
PROGRAM OF STRUCTURAL ENGINEERING**

**ADVISER
ASSIST. PROF. DR. SERKAN BEKIROĞLU**

ISTANBUL, 2017

ACKNOWLEDGEMENTS

I would like to thank Assist. Prof. Dr. Serkan Bekirođlu for encouraging me to do this research and for supervising my efforts. He generally knew which was appropriate at any given time and never stops pushing me forward.

Grateful for the treatment of high-end brotherly of all the staff of Civil Engineering in Yıldız Technical University.

I give it to my ambition father. I hope he was still there looking for my retaining back home.

Last but by no means least; I must record my deepest gratitude to the beautiful city that I will never forget it "Istanbul", it will live in my heart forever.

April, 2017

Hanan ALIMAM

TABLE OF CONTENTS

	Page
LIST OF SYMBOLS	x
LIST OF ABBREVIATIONS.....	xi
LIST OF FIGURES	xiii
LIST OF TABLES.....	xv
ABSTRACT	xvi
ÖZET	xvii
CHAPTER 1	
INTRODUCTION	1
1.1 Literature Review	1
1.1.1 Background of Finite Element Method (FEM)	1
1.1.2 Background of Functionally Graded Material (FGM)	2
1.1.3 Background about research on Finite Element Method (FEM) and Functionally Graded Material (FGM)	6
1.2 Objective of the Thesis	7
1.3 Hypothesis	8
CHAPTER 2	
A FINITE ELEMENT IMPLEMENTATION	9
2.1 Structural Modelling and FEM Analysis	9
2.1.1 Classification of the Problem.....	9
2.1.2 Conceptual, Structural and Computational Models.....	10
2.1.3 Structural Analysis by the FEM	11

2.1.4	Verification of FEM Results.....	12
2.2	Finite Element Procedure	13
2.2.1	Finite Element Discretization	14
2.2.2	Higher-Order Shape Functions	15
1-	A 4-Noded Quadrilateral Element.....	15
2-	A 8-Noded Quadrilateral Element.....	15
3-	A 17-Noded Quadrilateral Element.....	17
2.2.3	Formulation of the Stiffness Matrix	20
2.2.4	Stress / Strain Matrix (or Constitutive Matrix)	26
2.2.5	Evaluate a Line Distributed Load	28
2.2.6	Functionally Graded Material (FGM)	29
CHAPTER 3		
	PROGRAMMING THE FE-CODE	30
3.1	The Code Main Frame	30
3.1.1	Input Data	30
3.1.2	Compute Local Stiffness Matrix and Local Load Vector for Elements	30
3.1.3	Global Stiffness Matrix [K], and Global Load Vector [F]	33
3.2	Important Subroutine	33
3.2.1	Line Distributed Load.	33
3.2.2	Material Matrix [D] for FGM	35
CHAPTER 4		
	NUMERICAL PROBLEMS	37
4.1	Patch Test Group	38
4.1.1	First Patch Test	38
4.1.2	Second Patch Test.....	40
4.2	ABAQUS Program Group	43
4.2.1	A Retaining Wall	43

4.2.2 A Deformed Steel Beam	47
4.3 Functionally Graded Material (FGM) group	50
4.3.1 A retaining Wall with FGM.....	50
4.3.2 An Embedded Water Tank with FGM	54
CHAPTER 5	
CONCLUSION.....	58
REFERENCES	60
CURRICULUM VITAE.....	62



LIST OF SYMBOLS

Δk	Virtual kinetic energy
Ω	Material body or domain
U	Displacement field
Δu	Variation of displacement
a	Acceleration of system,
δW_{int}	Internal virtual work
$\Delta \varepsilon$	Variation of strain tensor,
σ	Cauchy stress tensor,
δW_{ext}	The external virtual work
P	Density
B	The body force
t^*	Vector on the surface of system
Γ_{σ}	Static boundary of domain
S, t	Natural coordinates for a quadrilateral element
U	Displacement in horizontal direction
V	Displacement in vertical direction
E	Strain
Q	Displacement vector

J	Jacobian
γ_{xy}	Shear strain
σ_x	Stress in x direction
τ_x	Shear stress
H	Thickness
K	Stiffness matrix
D	Constitutive or material matrix
E	Modulus of elasticity
ν	Poisson ratio
F	Force vector
P _e	The effective property
P ₁	The material property for material 1
P ₂	The material property for material 2
V ₁	The volume fractions of material 1
V ₂	The volume fractions of material 2

LIST OF ABBREVIATIONS

FEM	Finite Element Method
FGM	Functionally Graded Material
2D	Two dimension
3D	Three dimension

LIST OF FIGURES

	Page
Figure1.1	Fields of applications for FGM..... 2
Figure1.2	Based on nature of gradients, different types of Functionally Graded Materials may be of (a) fraction gradient type, (b) shape gradient type,(c) orientation gradient type, and (d) size gradient type..... 3
Figure1.3	Global gradation (a) Continuous and (b) stepwise graded structures..... 5
Figure1.4	Local gradient at the (a) surface and (b) joint..... 5
Figure2.1	A computational model for the analysis of a structure..... 13
Figure 2.2	Quadrilateral coordinates..... 14
Figure 2.3	4-noded quadrilateral element used in this study 14
Figure 2.4	8-noded quadrilateral element used in this study 16
Figure 2.5	17-noded quadrilateral element used in this study 19
Figure 2.6	The FGM model in this study..... 29
Figure 3.1	Flowchart of the FE-code..... 31
Figure 3.2	Flowchart of computing local stiffness matrix [k], and local load vector [f] for elements..... 32
Figure 3.3	Flowchart of computing global load vector [F] from line load..... 34
Figure 3.4	Computing material matrix [D]for FGM..... 35
Figure 4.1	Geometry, load pattern, and mesh of Patch problem..... 37
Figure 4.2	The deformed shape of Patch problem..... 38
Figure 4.3	Geometry, load pattern, and mesh of Patch problem..... 40
Figure 4.4	The deformed shape of Patch problem..... 40

Figure 4.5	a) Mesh structure of the retaining wall within ABAQUS, and b) Mesh, load pattern, and geometry of the FE-code.....	43
Figure 4.6	The deformed shapes for the retaining wall within a) ABAQUS and b) The FE-code.....	44
Figure 4.7	Displacement results for the retaining wall.....	46
Figure 4.8	Stress results for the retaining wall.....	46
Figure 4.9	The deformed steel beam section.....	47
Figure 4.10	The supporting and loading points of the deformed steel beam.....	48
Figure 4.11	The deformed shapes for the beam within a) ABAQUS and b) The FE-code.....	48
Figure 4.12	Load pattern, geometry, and material property of the retaining wall with FGM.....	50
Figure 4.13	Mesh structure of the retaining wall with FGM.....	51
Figure 4.14	The deformed shape of retaining wall with FGM for 4-noded element..	51
Figure 4.15	Displacement results for the retaining wall with FGM.....	53
Figure 4.16	Stress results for the retaining wall with FGM.....	53
Figure 4.17	Structure dimensions for an embedded water tank.....	54
Figure 4.18	Mesh structure of an embedded water tank.....	55
Figure 4.19	The deformed shapes for the embedded water tank.....	55
Figure 4.20	Displacement results for the embedded water tank.....	57
Figure 4.21	Stress results for the embedded water tank.....	57

LIST OF TABLES

	Page
Table 4.1 Comparisons of displacement results for 4-noded; 8-noded; 17-noded elements with the results given in literature	38
Table 4.2 Comparisons of stress results for 4-noded; 8-noded; 17-noded elements with the results given in literature.....	39
Table 4.3 Comparisons of displacement results for 4-noded; 8-noded; 17-noded elements with the results given in literature.....	41
Table 4.4 Comparisons of stress results for 4-noded; 8-noded; 17-noded elements with the results given in literature.....	41
Table 4.5 Comparison of results of the FE-code for retaining wall with non-FGM and ABAQUS.....	44
Table 4.6 Displacement and stress results of retaining wall with FGM.....	52
Table 4.7 Displacement and stress results of the embedded water tank.....	56

ABSTRACT

FINITE ELEMENT ANALYSIS OF STRUCTURAL PROBLEMS WITH FUNCTIONALLY GRADED MATERIAL USING HIGHER ORDER ELEMENTS

Hanan ALIMAM

Department of Civil Engineering

MSc. Thesis

Adviser: Assist Prof. Dr. Serkan Bekiroğlu

Applications of Functionally Graded Materials (FGMs) are very interesting, because of flexibility to make the composite material for many implementation requirement and functional suitability.

This study is motivated to develop a finite element code, with high accuracy, by using higher order elements. This FE-code will have the ability of dealing with Functionally Graded Materials (FGMs).

Shape functions of higher order element which are used in discretization of geometry and displacement field lead to higher order strain variations in a finite element and satisfy convergence throughout the exact solution with fewer elements.

The FE-code will consist of a 4-, 8-, and 17-noded quadrilateral finite elements. In order to get a more complete view, numerical results are achieved and verified for different problems to show accuracy and reliability of the FE-code. The given results in literature as exact and numerical values of some problems and the finite element software ABAQUS program will be used to compare results.

FE-code will be applied to main problems which consist of two structural problems made of a Functionally Graded Material (FGM). In the analysis of these structural problems, the gradient region is in the horizontal direction.

Chapter one will give a literature review about FEM, FGM, and the research done in them. Chapter two will deal with general information about FEM and FGM while chapter three, will explain equations and their derivatives. Moreover, it will illustrate the important part of FE-code programming. Chapter four will show the numerical

problems and their results. Finally, chapter five will give the conclusion of the study and the future work related to it.

Key words: Functionally Graded Material (FGM), Finite Element, Matlab language, ABAQUS program, 4-noded, 8-node, 17-noded.



YILDIZ TECHNICAL UNIVERSITY
GRADUATE SCHOOL OF NATURAL AND APPLIED SCIENCES

**YÜKSEK DERECELİ ELEMANLAR KULLANARAK
FONKSİYON KADEMELİ MALZEMEYE SAHİP YAPISAL
PROBLEMLERİN SONLU ELEMAN ANALİZLERİ**

Hanan AİMAN

İnşaat Mühendisliği

Yüksek Lisans Tezi

Danışman: Yrd. Doç. Dr. Serkan BEKİROĞLU

Fonksiyon kademeli malzemelerin uygulamaları, birçok uygulama ihtiyacı ve fonksiyonel uygunluk için kompozit malzeme oluşturmanın getirdiği kolaylık nedeniyle ilgi çekicidir.

Bu çalışma yüksek dereceli elemanlar kullanarak yüksek doğruluklu sonlu elemanlar geliştirmeyi hedeflemektedir. Geliştirilecek sonlu eleman kodu fonksiyon kademeli malzeme tanımının yapılmasına imkan sağlayacaktır.

Yerdeğiştirme ve geometrinin ayrıklaştırılmasında kullanılan yüksek dereceli elemanların şekil fonksiyonları, sonlu elemanlarda şekil değiştirme değişimini elde etmeyi ve birkaç eleman ile analitik çözüme yakınsamayı sağlar.

Sonlu eleman kodu 4, 8 ve 17 noktalı dörtgen sonlu elemanlardan oluşacaktır. Geliştirilen sonlu elemanın güvenilirliği ve doğruluğunu göstermek için farklı problemler çözülerek sayısal sonuçlar elde edilecek ve doğrulanacaktır. Bazı problemlerin literatürde verilen analitik ve nümerik sonuçları ile ABAQUS sonlu eleman yazılımının sonuçları karşılaştırma için kullanılacaktır.

Sonlu eleman kodu, fonksiyon kademeli malzeme tanımının kullanıldığı iki ana yapısal probleme uygulanacaktır. Bu yapısal problemlerin analizinde, malzeme özelliği değişimi yatay yönde olacaktır.

Birinci bölümde sonlu eleman metodu ve fonksiyon kademeli malzeme hakkında literatür verilecektir. İkinci bölümde sonlu eleman metodu fonksiyon kademeli malzeme hakkında genel bilgileri içerecektir. Üçüncü bölümde ise denklemler ve bağıntılar elde edilecektir. Ayrıca bu bölümde sonlu eleman kodu ile ilgili önemli kısımlar sunulacaktır. Dördüncü bölüm, sayısal örnekleri ve sonuçlarını sunacaktır. Son olarak beşinci bölüm, çalışmanın sonuçlarını içerecektir.

Anahtar Kelimeler: Fonksiyon Kademeli Malzemeli, Sonlu Eleman, Matlab program, ABAQUS program, 4 , 8 ve 17 noktalı.



INTRODUCTION

1.1 Literature Review

1.1.1 Background of Finite Element Method (FEM)

In last three decades, the finite element method practiced on the computers has been used effectively in modelling complex issues in different engineering zones and has enlarged the chance of safe and cost effective design.

The successful use of the FEM is possible only if the essential assumptions of the strategies used are known, and the strategy can be practiced confidently on the PC.

In this method, the geometry of a structure is discretized when it is divided into a mesh of finite elements of certain accuracy. Clearly, the discretization enters another approximation. So, there are two error sources from the outset: the modelling error and the discretization error [1]. The discretization error, on the other hand, can be decreased by using a smaller mesh which means more elements, or else by increasing the accuracy using higher order polynomial expansions for approximating the displacement field within each element as what will be done in this study.

Higher order element shape functions can be developed by adding extra nodes to the sides of the linear element. These elements lead to higher-order strain variations in every element, and convergence to the exact solution with fewer elements [2].

William F. Mitchell studied the magnitude of how much a polynomial degree is beneficial to high order and confirmed that for high accuracy demands, higher order elements are appropriate [3].

FEM and related techniques can help for making the complex engineering applications to easier one. It has been certified that the numerical approaches, especially FEM and related techniques are able to handle a wide range of engineering problems, and offer unlimited

advantages over conventional numerical methods, specifically for the problems with discontinuities and large deformation. The Finite Element Model relatively easily and cheaply. In addition to its ability to deal with different load conditions without difficulty and, with multi types and numbers of boundary conditions, it can model irregularly shaped bodies not complexly, deal with dynamic effects effectively, change the size of the elements to make it possible to use small elements where ever it needs, and deal with nonlinear behavior existing with large deformations and nonlinear materials.

The most important property that serves our study is the potential to model momentous composed of several different materials because the element equations are evaluated individually [2].

1.1.2 Background of Functionally Graded Material (FGM)

As technology progresses go in increasing rate, the need for advanced capability materials becomes a main priority in the engineering needs of more complex and higher performance systems. This demand can be seen in a lot of fields in which engineers are exploring the applications of these new engineered materials, fields of applications for Functionally Graded Material (FGM) are illustrated in Figure 1.1.

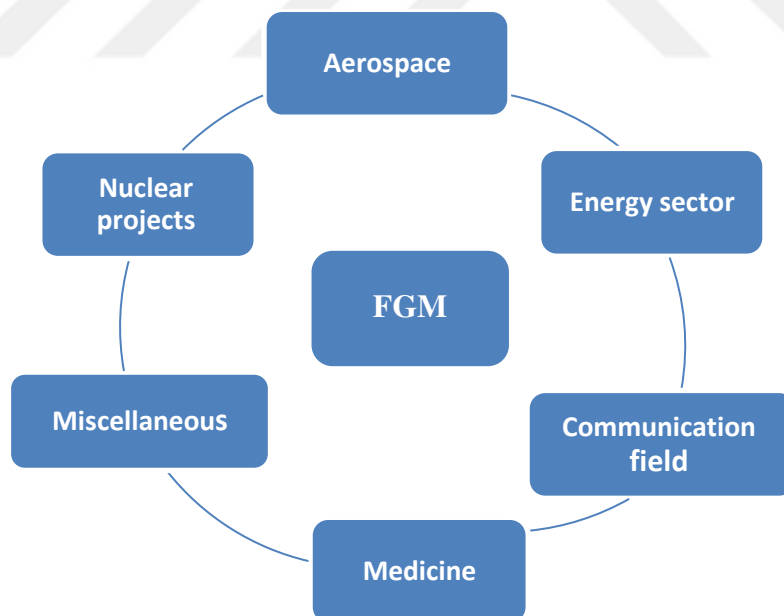


Figure 1.1 Fields of applications for FGM [4]

Functionally Graded Material (FGM) belongs to a class of advanced material characterized by variation in properties as the dimension varies. These materials are a modern generation of engineered materials that are getting interested in last years. The overall properties of FGM are unique and varies from any of the individual material that forms it. They were

initially proposed by a group of Japanese aerospace scientists for structural applications and fusion reactors [5].

The FGM was proposed to prepare a new composite by utilizing heat-resistant ceramics on the high-temperature side and hard metals with a strong thermal conductivity on the other side (low temperature), with a gradient material variation from ceramic to metal [6].

Depending on the gradient type, the FGM might be gathered as appeared in Figure 1.2:

- Fraction gradient type Figure 1.2a.
- Shape gradient type Figure 1.2b.
- Orientation gradient type Figure 1.2c.
- Size (of material) gradient type Figure 1.2d.

And according to number of directions the properties changed, we can sort as 1-dimensional, 2- dimensional or 3-dimensional FGM.

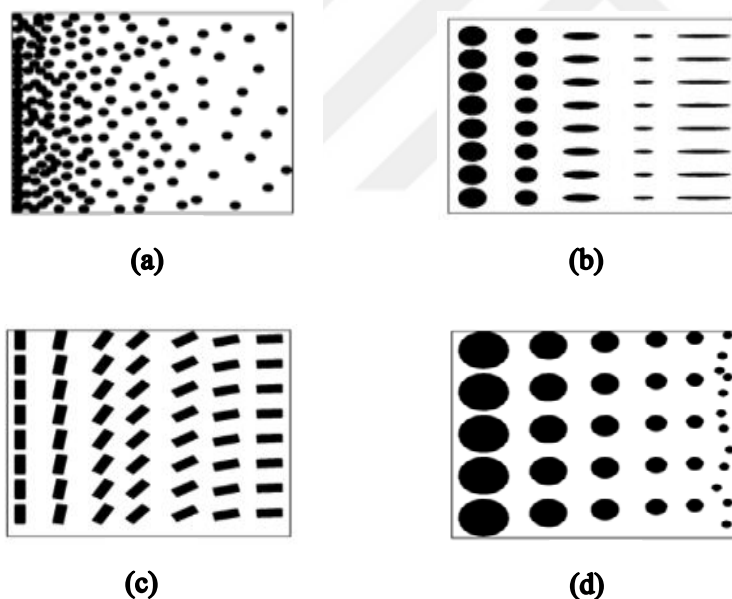


Figure 1.2 Based on nature of gradients, different types of Functionally Graded Materials may be of (a) fraction gradient type, (b) shape gradient type, (c) orientation gradient type, and (d) size gradient type [5].

The two essential structures of gradient are outlined in Figure 1.3. For the continuously graded structure, two diverse material stages steadily change starting with one side then onto the next, as appeared in Figure 1.3(a); while in Figure 1.3 (b), material stages change in a broken way, for example, a stepwise gradation which is likewise called segmented FGMs. The spatial gradation may display at a global or local level. In a global gradation

(Figure 1.3), the variety of properties reaches out over the main part of the material. Despite what might be expected, local gradation is limited to a specific area in the material, for example, covering at first glance or joint in the interfacial district as in Figure 1.4 [7].

Some of the advantages of Functionally Graded Materials are [4]:

- FGM as an interface layer to associate two contradictory materials can incredibly improve the bond strength.
- FGM are utilized in energy conversion device.
- FGM covering and interface can be utilized to decrease the residual stress and thermal stress.
- FGM additionally gives the chances to take the advantages of various material frameworks.
- FGM covering can be utilized to associate the materials to get rid of the stress at the interface and endpoint stress feature.
- FGM covering improves the strength of the associations as well as lessen the crack driving force.
- FGM can control deformation, wear, corrosion dynamic response, and so on.
- FGM has extensive variety of uses in dental and orthopaedic applications for teeth and bone substitution.

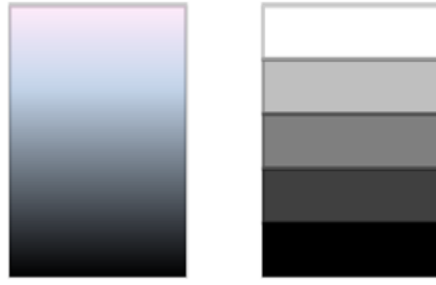


Figure 1.3 Global gradation (a) continuous and (b) stepwise graded structures [7].



Figure 1.4 Local gradient at the (a) surface and (b) joint [7].

There are a few issues that need further review and to be fixed, primarily in the accompanying points [4]:

- A right database of gradient material (counting material framework, parameters, material readiness and execution assessment) is to be expanded.
- Studies ought to concentrate on variety of gradient material as for thermal stress relaxation of the material and also for different fields of engineering applications.
- Until now, it requires further research and examination on the physical properties of the material model. Macroscopic unit of structure and the quantitative relationship between planning conditions to be built up with a specific end goal to carefully and dependable foretell the physical properties of graded materials.
- Functionally gradient materials arranged for tests are specimen with little size and purely structure. It needs more practical results.
- The planning expenses are high.
- Requires enhancing the continuum theory, quantum (discrete) theory, percolation theory and microstructure model, and depending on computer simulation of the material properties for specific theoretical expectation.

1.1.3 Background about Research on Finite Element Method (FEM) and Functionally Graded Material (FGM)

Many of research in the FGM has been completed until now. Hong-Tian Xiao and Zhong-Qi Yue [8] studied stresses and displacements in Functionally Graded Materials of semi-infinite extent induced by uniform distributed load. They analysed the stress and displacement fields in a FGM of semi-infinite motivated from uniform distributed loading. They got a high accuracy numerical integration results.

Another study was made by B.L. Shao [9], he established an axisymmetric and isoparametric graded element to model the functionally graded circular piezoelectric plates using coarse mesh, where MATLAB was used to implement the whole FEM code. Numerical examples were presented to verify their method.

K. Sanjay [10] worked on free vibration analysis of functionally graded beams, carried out for various classical boundary conditions, found that for the real structures with less length to thickness ratios, transverse shear effects should be included to predict accurate careful frequencies and mode shapes for homogenous and FGM beams.

Makwana B. [11], studied the stress of Functionally Graded Material for a plate with cut-out, where general solutions are obtained with MATLAB coding and compared with an FEA tool (ANSYS). The code checked the effect of stress concentration effect for scaled modelling of object with different scale factors.

Bhandari M. [12], studied the mechanical deformation of FGM of ceramic-metal plates under various boundary conditions. His results shown a satisfying result with those available in the literature and the bending response of the FG plate is intermediate to those of the metal and the ceramic plate.

Another study was made by S. Natarajan [13]. It was about analysis of FGM plates with triangular elements and cell-based smoothed discrete shear gap process. It was concerned on the static bending, free vibration, and mechanical and thermal buckling behavior of FGM plates. He improved that finite element method shows insensitivity to shear locking and produces good results in static bending, free vibration, and buckling of FG plates.

1.2 Objective of the Thesis

The basic objective of this thesis is to develop a finite element code (FE-code) with higher order shape function. The FE-code will consist of a 4-, 8-, and 17-noded quadrilateral finite elements. It must have a qualified accuracy, facilitated to use, clear enough to make developer easily recognize the geometry, boundary conditions definition, and results interpretation.

The second objective of the FE-code is to solve Functionally Graded Material (FGM) problems with an adequate accuracy depending on these higher order shape function.

In summary, the objectives of this thesis can mainly be articulated as follows:-

- Create a finite element code with higher order shape function. The FE-code will consist of a 4-, 8-, and 17-noded quadrilateral finite elements.
- Generalize the code to solve many structural types (especially Functionally Graded Materials (FGMs) which represent our main problem).
- By using a common language, simply the FE-code to recognize the geometric, boundary conditions definition, and results interpretation.
- Understandable to realize the results and errors if occurs.
- Improve it to have high accuracy for results as possible.
- Because it is often difficult or costly to make direct measurements for FGM, this FE-code simplifies that issue.
- It solved the main problem of our study which represent a FGM problems after the FE-code has been verified with many problems and compared their results with the results given in literature as exact and numerical values for some problems and with the ABAQUS in others problems.

1.3 Hypothesis

An effective computational approach using MATLAB program, based on a high order polynomial is proposed for the analysis of a special structural problem which is mainly made of Functionally Graded Materials (FGMs). Material properties of FGM are assumed to vary through the axial direction under the power law [14]. Numerical outcomes are computed and verified to demonstrate the accuracy and reliability of the present code. This analytical model allows the material properties be a continuous function along the axial direction of the continuum.



CHAPTER 2

A FINITE ELEMENT IMPLEMENTATION

2.1 Structural Modelling and FEM Analysis

The Finite Element Method (FEM) is a system for the numerical arrangement of the equations that ruled the issues found in nature. Normally the behavior of nature can be showed by equations as differential or integral form. For this reason, the FEM is understood in mathematical fields as a numerical technique for solving partial differential or integral equations.

At the point of referring to the analysis of structures, the FEM is an effective strategy for processing the displacements, stresses and strains in a structure under an arrangement of loads.

A finite element can be pictured as a little portion of a structure. The word "finite" recognizes such a portion from the "infinitesimal" elements of differential calculus. The geometry of the structure is considered to be formed by the get together of an accumulation of non-overlapping domains with simple geometry termed finite elements. Triangles and quadrilaterals in two dimensions (2D) or tetrahedral and hexahedra in three dimensions (3D) are ordinarily shown to the "elements". It is usually said that a "mesh" of finite elements "discretizes" the structure.

2.1.1 Classification of the Problem

The first step in the solution of a problem is to identify the problem itself. Hence, before we can analyse a structure we must answer these questions:

- What are the more relevant physical phenomena influencing the structure?
- Is the problem in static or dynamic nature?
- Is the kinematics or the material properties linear or non-linear?
- Which are the key results requested?
- What is the level of accuracy expected?
- The answers to these questions are basic for selecting a structural model and the sufficient computational method.

2.1.2 Conceptual, Structural and Computational Models

Computational methods like the FEM are utilized to calculate models of an essential problem, and not to the real problem itself. Indeed, even test methods in structural research centers make utilization of scale generations of the theoretical model picked (likewise called physical models) unless the real structure is tried in essential size, which rarely happens.

A conceptual model can be produced once the physical way of a problem is clearly understood. In the derivation of a conceptual model worked must exclude unnecessary details and include all the concerned features of the problem under consideration so that the model can describe reality with sufficient accuracy. A conceptual model for a problem should include all the data necessary for its acting and analysis.

Obviously another person will have another perception of reality and, consequently, the conceptual model for the same structure can take different forms.

Subsequent to selecting a conceptual model of a structure, the next step for the numerical (and analytical) study is the definition of a structural model (sometimes called mathematical model).

A structural model must include three basic aspects: The geometric description of the structure by means of its geometrical ingredients (points, lines, surfaces, volumes), the mathematical expression of the basic physical laws ruling the behavior of the structure (i.e. the force-equilibrium equations and the boundary conditions) usually written in terms of differential and/or integral equations, and the specification of the properties of the materials and of the forces acting on the structure.

Clearly, the conceptual model of a structure can be analysed using various structural models depending on the accuracy and/or simplicity sought in the analysis.

Every structural model provides a various set out for the analysis of the actual structure. A wrong conceptual or structural model will be a wrong solution, far from correct physical values, even if obtained with the most accurate numerical method [15].

The next step in the structural analysis sequence is to determine a numerical method, such as the FEM. The application of the finite element always demands its implementation in a computer code. The analysis of a structure with the FEM shows feeding the code with quantitative data for the mechanical properties of the materials, the boundary conditions and the applied loads (physical parameters) and in addition, the components of the discretization chosen (element type, mesh size, etc.).

The result of this procedure is a computational model for the analysis of a structure (Figure 2.1).

2.1.3 Structural Analysis by the FEM

The geometry of a structure is discretized when it is divided into a mesh of finite elements of certain accuracy. Clearly, the discretization enters another approximation. That means we have two error sources from the outset: the modelling error and the discretization error.

The former can be minimized by improving the conceptual and structural models which describe the actual behavior of the structure, as previously explained. The discretization error, on the other hand, can be minimized by using a smaller mesh (use more elements), or else by increasing the accuracy of the finite elements chosen using higher order polynomial expansions for approximating the displacement field within each element.

Additionally, the utilization of computers enters numerical errors associated with their ability to act data accurately with numbers of finite precision. The numerical error is always small, although it can be big in little problems, such as when some parts of the structure have very various physical properties.

The total of discretization and numerical errors add to the error of the computational model. Note that even if the computational error minimized to zero, it will not able to reproduce accurately of the actual behavior of the structure, unless the conceptual and structural models were perfect [15].

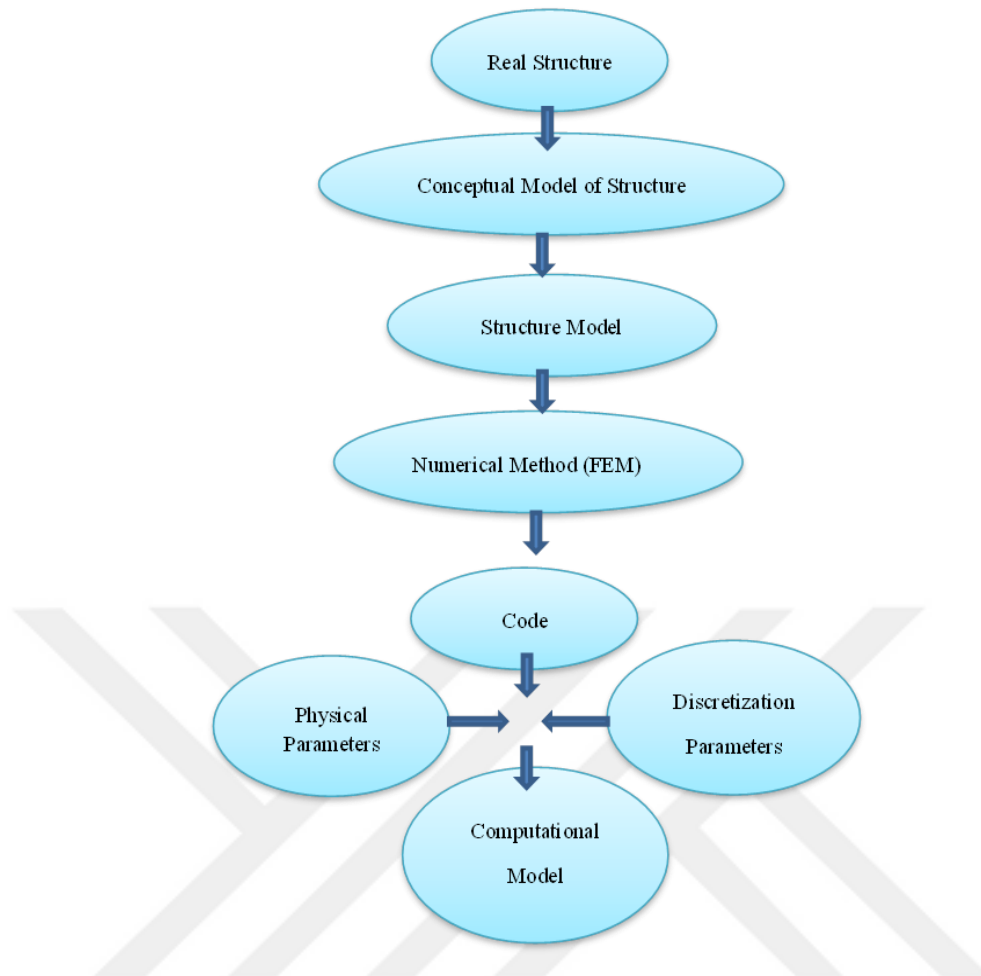


Figure 2.1 A computational model for the analysis of a structure [15].

2.1.4 Verification of FEM Results

Designers of structural FEM computer codes, analysts who use the codes and leaders who rely on the results of the analysis face a critical question: "How should confidence in modelling and computation be critically assessed?"

Verification of FEM results are the essential strategies for making and evaluating this certainty. Basically, verification is the process of determining that a computational model accurately represents the basic structural model and its solution.

In verification, thus, the relationship between the numerical results to the real world is not a case. The verification of FEM results is done by comparing the numerical results for simple benchmark problems with "exact" solutions get analytically, utilizing more accurate numerical methods.

A careful examination of the verification process indicates that there are two key parts of verification:

- Code verification, in order to build confidence that the mathematical model and the solution algorithms are working properly.
- Calculation verification aiming to build confidence that the separate solution of the mathematical model is accurate.

Among the code verification techniques, the well-known one is to compare code results with analytical solutions. As the number of such solutions is very limited, a code verification procedure with the ability to greatly widen is the use of manufactured solutions.

2.2 Finite Element Procedure

The principle of virtual work may create the procedure for finite element. An equation is produced with three terms:

- Virtual kinetic energy.

$$\delta K = \int_{\Omega} \delta u \cdot a \cdot dV \quad (2.1)$$

- Internal virtual work.

$$\delta W_{int} = \int_{\Omega} \delta \varepsilon : \sigma \cdot dV \quad (2.2)$$

- The external virtual work.

$$\delta W_{ext} = \int_{\Omega} \delta u \cdot b \cdot \rho \cdot dV + \int_{\Gamma_{\sigma}} \delta u \cdot t^* \cdot dA \quad (2.3)$$

These terms made the principle of virtual work equation:

$$\delta K + \delta W_{int} = \delta W_{ext} \quad (2.4)$$

Where δK is virtual kinetic energy, Ω material body or domain, u displacement field, δu variation of displacement, a acceleration of system, δW_{int} internal virtual work, $\delta \varepsilon$ variation of strain tensor, σ Cauchy stress tensor, δW_{ext} the external virtual work, ρ density, b the body force, t^* vector on the surface of system, Γ_{σ} static boundary of domain [16].

2.2.1 Finite Element Discretization

One of the essential steps in a finite element analysis is the discretization of a continuous body containing an infinite number of points on the surface into a discrete model with a limited number of nodes in the surface. The shape of the body between these nodes is approximated by functions. These functions are known as shape functions, which gives the ability to relate the coordinates of every point of a finite element with the locations of its nodes.

Quadratic elements are used in this FE-code. These elements are preferred for stress analysis, due to their high level of accuracy and their flexibility in modelling complex geometry, such as curved boundaries.

In order to present the quadratic element an appropriate natural coordinate system for that geometry must be used. The natural coordinates for a quadrilateral element (s, t) which are illustrated in Figure 2.2 are attached to the element, within the origin at the center of element.

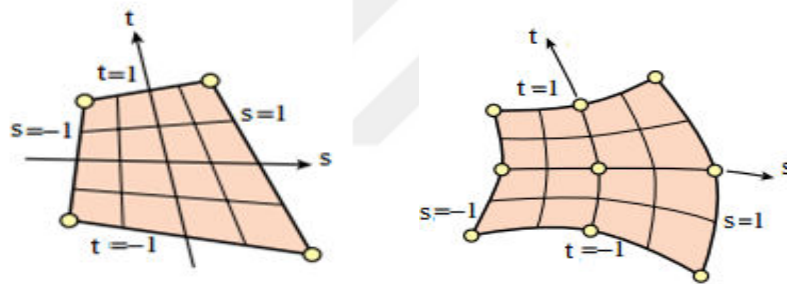


Figure 2.2 Quadrilateral coordinates [17]

These coordinates vary from -1 on one side to $+1$ at the other, taking the value zero over the quadrilateral medians. In this way, it converts the actual element as in Figure 2.3.

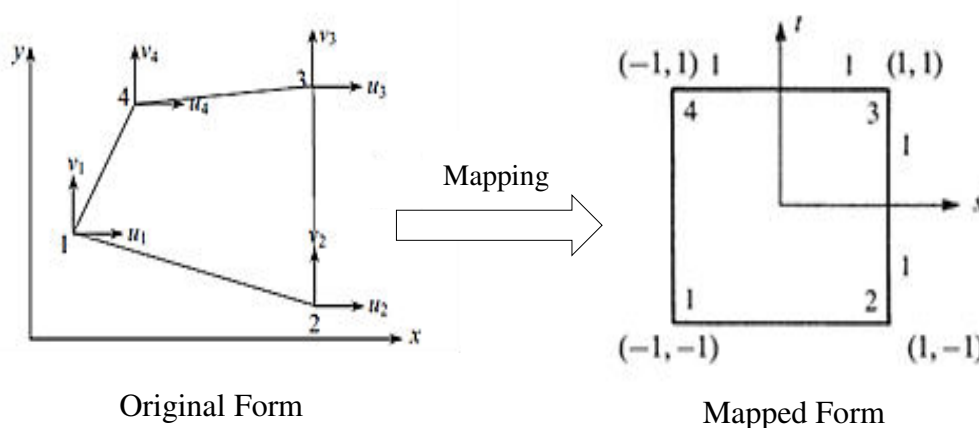


Figure 2.3 4-noded quadrilateral element used in this study [18].

2.2.2 Higher-Order Shape Functions

Higher-order element shape functions can be developed by adding extra nodes to the sides of the linear element. These elements lead to higher-order strain variations in every element, and convergence to the exact solution with fewer elements [2].

In this study, three different order of the polynomial is used. Firstly, a 4-noded element shown in Figure 2.3 is considered. Secondly, an 8-noded element shown in Figure 2.4 is considered. Finally, a 17-noded element shown in Figure 2.5 is considered.

1- A 4-Noded Quadrilateral Element

Shape functions of the 4-noded quadrilateral element are given below.

$$\begin{aligned}N1 &= 1/4 \times (1 - s) \times (1 - t) \\N2 &= 1/4 \times (1 + s) \times (1 - t) \\N3 &= 1/4 \times (1 + s) \times (1 + t) \\N4 &= 1/4 \times (1 - s) \times (1 + t)\end{aligned}\tag{2.5}$$

Moreover, their derivatives are given below.

$$\begin{aligned}\partial N1 / \partial s &= -(1 - t) / 4 \\ \partial N2 / \partial s &= (1 - t) / 4 \\ \partial N3 / \partial s &= (1 + t) / 4 \\ \partial N4 / \partial s &= -(1 + t) / 4 \\ \partial N1 / \partial t &= -(1 - s) / 4 \\ \partial N2 / \partial t &= -(1 + s) / 4 \\ \partial N3 / \partial t &= (1 + s) / 4 \\ \partial N4 / \partial t &= (1 - s) / 4\end{aligned}\tag{2.6}$$

2- A 8-Noded Quadrilateral Element

Shape functions of the 8-noded quadrilateral element are given below.

$$\begin{aligned}N1 &= 1/4 \times (1 - s) \times (1 - t) \times (-s - t - 1) \\N2 &= 1/4 \times (1 + s) \times (1 - t) \times (s - t - 1) \\N3 &= 1/4 \times (1 + s) \times (1 + t) \times (s + t - 1)\end{aligned}\tag{2.7}$$

$$\begin{aligned}
N4 &= 1/4 \times (1 - s) \times (1 + t) \times (-s + t - 1) \\
N5 &= 1/2 \times (1 - s^2) \times (1 - t) \\
N6 &= 1/2 \times (1 + s) \times (1 - t^2) \\
N7 &= 1/2 \times (1 - s^2) \times (1 + t) \\
N8 &= 1/2 \times (1 - s) \times (1 - t^2)
\end{aligned} \tag{2.7}$$

Moreover, their derivatives are given below.

$$\begin{aligned}
\partial N1 / \partial s &= (2s - t^2 - 2st + t) / 4 \\
\partial N2 / \partial s &= (2s + t^2 - 2st - t) / 4 \\
\partial N3 / \partial s &= (2s + t^2 + 2st + t) / 4 \\
\partial N4 / \partial s &= (2s - t^2 + 2st - t) / 4 \\
\partial N5 / \partial s &= (-2s + 2st) / 2 = s(t - 1) \\
\partial N6 / \partial s &= (1 - t^2) / 2 \\
\partial N7 / \partial s &= (-1 + t^2) / 2 = (t^2 - 1) / 2 \\
\partial N8 / \partial s &= (t^2 - 1) / 2 \\
\partial N1 / \partial t &= (-2st + 2t - s^2 + s) / 4 \\
\partial N2 / \partial t &= (2st + 2t - s^2 - s) / 4 \\
\partial N3 / \partial t &= (2st + 2t + s^2 + s) / 4 \\
\partial N4 / \partial t &= (-2st + 2t + s^2 - s) / 4 \\
\partial N5 / \partial t &= (s^2 - 1) / 2 \\
\partial N6 / \partial t &= (-2st - 2t) / 2 = -t(1 + s) \\
\partial N7 / \partial t &= (1 - s^2) / 2 \\
\partial N8 / \partial t &= (2st - 2t) / 2 = t(s - 1)
\end{aligned} \tag{2.8}$$

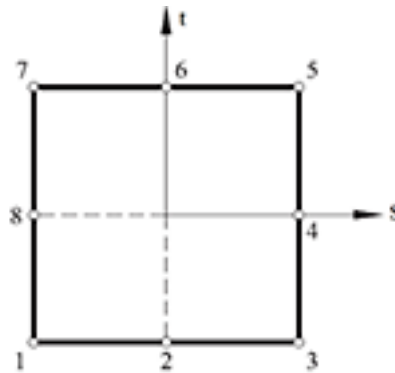


Figure 2.4 8-noded quadrilateral element used in this study [6].

3- A 17-Noded Quadrilateral Element

Shape functions of the 17-noded quadrilateral element are given below.

$$\begin{aligned}
 N1 &= 1/12 \times (1-s) \times (1-t) \times [4 \times (s^2-1) \times (-s) + 4 \times (t^2-1) \times (-t) \\
 &\quad + 3 \times s \times t] \\
 N2 &= 4/3 \times (1-t) \times (1-s^2) \times (s^2-s/2) \\
 N3 &= 2 \times (1-t) \times (s^2-1) \times (s^2+t/4) \\
 N4 &= 4/3 \times (1-t) \times (1-s^2) \times (s^2+s/2) \\
 N5 &= 1/12 \times (1+s) \times (1-t) \times [4 \times (s^2-1) \times s + 4 \times (t^2-1) \times (-t) \\
 &\quad - 3 \times s \times t] \\
 N6 &= 4/3 \times (1+s) \times (1-t^2) \times (t^2-t/2) \\
 N7 &= 2 \times (1+s) \times (t^2-1) \times (t^2-s/4) \\
 N8 &= 4/3 \times (1+s) \times (1-t^2) \times (t^2+t/2) \\
 N9 &= 1/12 \times (1+s) \times (1+t) \times [4 \times (s^2-1) \times s + 4 \times (t^2-1) \times t \\
 &\quad + 3 \times s \times t] \\
 N10 &= 4/3 \times (1+t) \times (1-s^2) \times (s^2+s/2) \\
 N11 &= 2 \times (1+t) \times (s^2-1) \times (s^2-t/4) \\
 N12 &= 4/3 \times (1+t) \times (1-s^2) \times (s^2-s/2) \\
 N13 &= 1/12 \times (1-s) \times (1+t) \times [4 \times (s^2-1) \times (-s) + 4 \times (t^2-1) \times t \\
 &\quad - 3 \times s \times t] \\
 N14 &= 4/3 \times (1-s) \times (1-t^2) \times (t^2+t/2) \\
 N15 &= 2 \times (1-s) \times (t^2-1) \times (t^2+s/4) \\
 N16 &= 4/3 \times (1-s) \times (1-t^2) \times (t^2-t/2) \\
 N17 &= (1-s^2) \times (1-t^2)
 \end{aligned} \tag{2.9}$$

Moreover, their derivatives are given below.

$$\begin{aligned}
 \partial N1 / \partial s &= 1/3 - 5/12 \times t - 2/3 \times s + 1/6 \times s \times t + 1/12 \times t^2 - s^2 + s^2 \times t \\
 &\quad + 1/3 \times t^3 + 1/2 \times s \times t^2 + 4/3 \times s^3 - 4/3 \times s^3 \times t \\
 &\quad - 1/3 \times t^4 + 4/3 \times s^3 \\
 \partial N2 / \partial s &= -2/3 + 2/3 \times t + 8/3 \times s - 8/3 \times s \times t + 2 \times s^2 - 2 \times s^2 \times t \\
 &\quad - 16/3 \times s^3 + 16/3 \times s^3 \times t \\
 \partial N3 / \partial s &= -4 \times s + 5 \times s \times t - s \times t^2 + 8 \times s^3 - 8 \times s^3 \times t
 \end{aligned} \tag{2.10}$$

$$\begin{aligned}
\partial N4/\partial s &= 2/3 - 2/3xt + 8/3xs - 8/3xst - 2xs^2 + 2xs^2xt \\
&\quad - 16/3xs^3 + 16/3xs^3xt \\
\partial N5/\partial s &= -1/3 + 5/12xt - 2/3xs + 1/6xst - 1/12xt^2 + s^2 - s^2xt \\
&\quad - 1/3xt^3 + 1/2xst^2 + 4/3xs^3 - 4/3xs^3xt \\
&\quad + 1/3xt^4 \\
\partial N6/\partial s &= -2/3xt + 4/3xt^2 + 2/3xt^3 - 4/3xt^4 \\
\partial N7/\partial s &= 1/2 + s - 5/2xt^2 - sxt^2 + 2xt^4 \\
\partial N8/\partial s &= 2/3xt + 4/3xt^2 - 2/3xt^3 - 4/3xt^4 \\
\partial N9/\partial s &= -1/3 - 5/12xt - 2/3xs - 1/6xst - 1/12xt^2 + s^2 + s^2xt \\
&\quad + 1/3xt^3 + 1/2xst^2 + 4/3xs^3 + 4/3xs^3xt \\
&\quad + 1/3xt^4 \\
\partial N10/\partial s &= 2/3 + 2/3xt + 8/3xs + 8/3xst - 2xs^2 - 2xs^2xt \\
&\quad - 16/3xs^3 - 16/3xs^3xt \\
\partial N11/\partial s &= -4xs - 5xst - sxt^2 + 8xs^3 + 8xs^3xt \tag{2.10} \\
\partial N12/\partial s &= -2/3 - 2/3xt + 8/3xs + 8/3xst + 2xs^2 + 2xs^2xt \\
&\quad - 16/3xs^3 - 16/3xs^3xt \\
\partial N13/\partial s &= 1/3 + 5/12xt - 2/3xs - 1/6xst + 1/12xt^2 - s^2 - s^2xt \\
&\quad - 1/3xt^3 + 1/2xst^2 + 4/3xs^3 + 4/3xs^3xt \\
&\quad - 1/3xt^4 \\
\partial N14/\partial s &= -2/3xt - 4/3xt^2 + 2/3xt^3 + 4/3xt^4 \\
\partial N15/\partial s &= -1/2 + s + 5/2xt^2 - sxt^2 - 2xt^4 \\
\partial N16/\partial s &= 2/3xt - 4/3xt^2 - 2/3xt^3 + 4/3xt^4 \\
\partial N17/\partial s &= -2xs + 2xt^2xs \\
\partial N1/\partial t &= 1/3 - 5/12xs + 1/12xs^2 + 1/6xst - 2/3xt + 1/3xs^3 \\
&\quad + sxt^2 - t^2 + 1/2xs^2xt - 1/3xs^4 - 4/3xst^3 \\
\partial N2/\partial t &= 2/3xs - 4/3xs^2 - 2/3xs^3 + 4/3xs^4 \\
\partial N3/\partial t &= -1/2 + 5/2xs^2 + t - s^2xt - 2xs^4 \\
\partial N4/\partial t &= -2/3xs - 4/3xs^2 + 2/3xs^3 + 4/3xs^4 \\
\partial N5/\partial t &= 1/3 + 5/12xs + 1/12xs^2 - 1/6xst - 2/3xt - 1/3xs^3 \\
&\quad - sxt^2 - t^2 + 1/2xs^2xt - 1/3xs^4 + 4/3xst^3 \\
&\quad + 4/3xt^3 \\
\partial N6/\partial t &= -2/3 - 2/3xs + 8/3xst + 8/3xt + 2xst^2 + 2xt^2 \\
&\quad - 16/3xst^3 - 16/3xt^3 \\
\partial N7/\partial t &= -5xst - 4xt - s^2xt + 8xst^3 + 8xt^3
\end{aligned}$$

$$\begin{aligned}
\partial N_8 / \partial \mathbf{a} &= 2/3 + 2/3xs + 8/3xst + 8/3xt - 2xst^2 - 2xt^2 \\
&\quad - 16/3xst^3 - 16/3xs^3 \\
\partial N_9 / \partial \mathbf{a} &= -1/3 - 5/12xs - 1/12xs^2 - 1/6xst - 2/3xt + 1/3xs^3 \\
&\quad + sxt^2 + t^2 + 1/2xs^2xt + 1/3xs^4 + 4/3xst^3 \\
&\quad + 4/3xt^3 \\
\partial N_{10} / \partial \mathbf{a} &= 2/3xs + 4/3xs^2 - 2/3xs^3 - 4/3xs^4 \\
\partial N_{11} / \partial \mathbf{a} &= 1/2 - 5/2xs^2 + t - s^2xt + 2xs^4 \\
\partial N_{12} / \partial \mathbf{a} &= -2/3xs + 4/3xs^2 + 2/3xs^3 - 4/3xs^4 \\
\partial N_{13} / \partial \mathbf{a} &= -1/3 + 5/12xs - 1/12xs^2 + 1/6xst - 2/3xt - 1/3xs^3 \\
&\quad - sxt^2 + t^2 + 1/2xs^2xt + 1/3xs^4 - 4/3xst^3 \\
&\quad + 4/3xt^3 \\
\partial N_{14} / \partial \mathbf{a} &= 2/3 - 2/3xs - 8/3xst + 8/3xt + 2xst^2 - 2xt^2 \\
&\quad + 16/3xst^3 - 16/3xt^3 \\
\partial N_{15} / \partial \mathbf{a} &= 5xst - 4xt - s^2xt - 8xst^3 + 8xt^3 \\
\partial N_{16} / \partial \mathbf{a} &= -2/3 + 2/3xs - 8/3xst + 8/3xt - 2xst^2 + 2xt^2 + \\
&\quad 16/3xst^3 - 16/3xt^3 \\
\partial N_{17} / \partial \mathbf{a} &= -2xt + 2xs^2xt
\end{aligned} \tag{2.10}$$

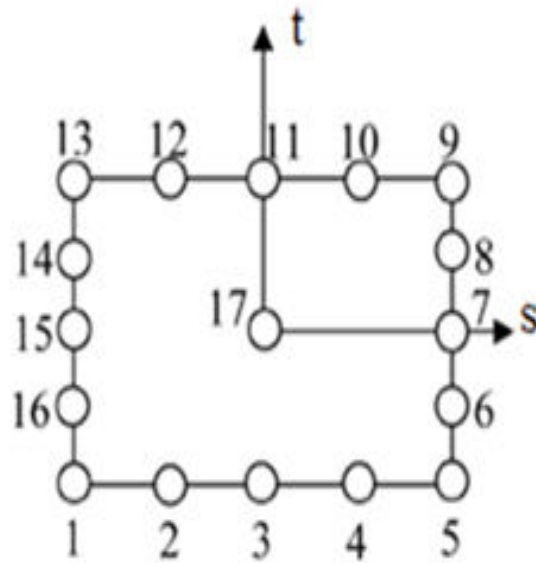


Figure 2.5 17-noded quadrilateral element used in this study [19].

2.2.3 Formulation of the Stiffness Matrix

Isoparametric Formulation of the Quadrilateral Element which is derived from the use of the same interpolation functions to define the element shape as are used to define the displacements within the element.

Step 1: Define the element geometric shape

For the special case when the distorted element becomes a rectangular element with sides parallel to the global x-y coordinates, the s-t coordinates can be related to the global element coordinates x, y by:

$$X = x_c + b_s \quad (2.11)$$

$$Y = y_c + h_t$$

Where x_c and y_c are the global coordinates of the element centroid. Assuming global coordinates x and y are related to the natural coordinates s and t as follows:

$$X = a_1 + a_2s + a_3t + a_4st \quad (2.12)$$

$$Y = a_1 + a_2s + a_3t + a_4st$$

Solving them will obtain:

$$X = \frac{1}{4} \times [(1-s) \times (1-t) \times x_1 + (1+s) \times (1-t) \times x_2 + (1+s) \times (1+t) \times x_3 + (1-s) \times (1+t) \times x_4]$$

$$Y = \frac{1}{4} \times [(1-s) \times (1-t) \times y_1 + (1+s) \times (1-t) \times y_2 + (1+s) \times (1+t) \times y_3 + (1-s) \times (1+t) \times y_4] \quad (2.13)$$

In matrix form:

$$\begin{Bmatrix} X \\ Y \end{Bmatrix} = \begin{bmatrix} N_1 & 0 & N_2 & 0 & N_3 & 0 & N_4 & 0 \\ 0 & N_1 & 0 & N_2 & 0 & N_3 & 0 & N_4 \end{bmatrix} \begin{Bmatrix} X_1 \\ Y_1 \\ X_2 \\ Y_2 \\ X_3 \\ Y_3 \\ X_4 \\ Y_4 \end{Bmatrix} \quad (2.14)$$

where:

$$\begin{aligned} N_1 &= \frac{(1-s)(1-t)}{4} & N_2 &= \frac{(1+s)(1-t)}{4} \\ N_3 &= \frac{(1+s)(1+t)}{4} & N_4 &= \frac{(1-s)(1+t)}{4} \end{aligned} \quad (2.15)$$

These shape functions are seen to map the s and t coordinates of any point in the square element to those x and y coordinates in the quadrilateral element.

Consider square element node 1 coordinates, where s = -1 and t = -1 then x = x1 and y = y1.

However, physical anticipation can often guide us into directly expressing shape functions based on the following two criteria and used on numerous occasions:

$$\sum_{i=1}^n N_i = 1 \quad i = 1, 2, 3, \dots, n \quad (2.16)$$

$$\begin{aligned} x &= \{N\}^T \{x_n\} \\ y &= \{N\}^T \{y_n\} \end{aligned} \quad (2.17)$$

Step 2: Displacement functions

The displacement functions within an element are now similarly defined by the same shape functions as are used to define the element geometric shape:

$$\begin{Bmatrix} u \\ v \end{Bmatrix} = \begin{bmatrix} N_1 & 0 & N_2 & 0 & N_3 & 0 & N_4 & 0 \\ 0 & N_1 & 0 & N_2 & 0 & N_3 & 0 & N_4 \end{bmatrix} \begin{Bmatrix} u_1 \\ v_1 \\ u_2 \\ v_2 \\ u_3 \\ v_3 \\ u_4 \\ v_4 \end{Bmatrix} \quad (2.18)$$

Where u, v are displacements in horizontal and vertical direction, respectively.

Step 3: Strain-Displacement and Stress-Strain Relationships

Element matrix [B] will formulate to evaluate an element stiffness matrix [k]. However, because it becomes difficult (if not impossible) to write the shape functions in terms of the

x and y coordinates, we will carry out the formulation in terms of the isoparametric coordinates s and t.

This may appear difficult, but it is easier to use the s- and t coordinate expressions. This approach also leads to a simple computer program formulation.

To construct an element stiffness matrix, we must determine the strains, which are defined in terms of the derivatives of the displacements with respect to the x and y coordinates. The displacements, however, are now functions of the s and t coordinates.

The derivatives $\partial u/\partial x$ and $\partial v/\partial y$ are now expressed in terms of s and t. Therefore, we need to apply the chain rule of differentiation. The chain rule yields:

$$\begin{aligned}\frac{\partial f}{\partial s} &= \frac{\partial f}{\partial x} \frac{\partial x}{\partial s} + \frac{\partial f}{\partial y} \frac{\partial y}{\partial s} \\ \frac{\partial f}{\partial t} &= \frac{\partial f}{\partial x} \frac{\partial x}{\partial t} + \frac{\partial f}{\partial y} \frac{\partial y}{\partial t}\end{aligned}\tag{2.19}$$

The strains ε_x can then be found; for example

$$\varepsilon_x = \partial u/\partial x\tag{2.20}$$

Using Cramer's rule

$$\frac{\partial f}{\partial x} = \frac{\begin{vmatrix} \frac{\partial f}{\partial s} & \frac{\partial y}{\partial s} \\ \frac{\partial f}{\partial t} & \frac{\partial y}{\partial t} \end{vmatrix}}{\begin{vmatrix} \frac{\partial x}{\partial s} & \frac{\partial y}{\partial s} \\ \frac{\partial x}{\partial t} & \frac{\partial y}{\partial t} \end{vmatrix}} = \frac{\begin{vmatrix} \frac{\partial x}{\partial s} & \frac{\partial f}{\partial s} \\ \frac{\partial x}{\partial t} & \frac{\partial f}{\partial t} \end{vmatrix}}{\begin{vmatrix} \frac{\partial x}{\partial s} & \frac{\partial y}{\partial s} \\ \frac{\partial x}{\partial t} & \frac{\partial y}{\partial t} \end{vmatrix}}\tag{2.21}$$

The determinant in the denominator is the determinant of the Jacobian matrix [J].

$$|J| = \begin{vmatrix} \frac{\partial x}{\partial s} & \frac{\partial y}{\partial s} \\ \frac{\partial x}{\partial t} & \frac{\partial y}{\partial t} \end{vmatrix}\tag{2.22}$$

We now want to express the element strains as:

$$\{\varepsilon\} = [B]\{q\}\tag{2.23}$$

Where [B] must now be expressed as a function of (s), and (t). The usual relationship between strains and displacements given in matrix form as:

$$\begin{aligned} \{\varepsilon\} &= \begin{Bmatrix} \varepsilon_x \\ \varepsilon_y \\ \gamma_{xy} \end{Bmatrix} = \begin{Bmatrix} \partial u / \partial x \\ \partial v / \partial y \\ \frac{\partial u}{\partial y} + \frac{\partial v}{\partial x} \end{Bmatrix} = \begin{Bmatrix} \partial(\cdot) / \partial x & 0 \\ 0 & \partial(\cdot) / \partial y \\ \partial(\cdot) / \partial y & \partial(\cdot) / \partial x \end{Bmatrix} \begin{Bmatrix} u \\ v \end{Bmatrix} \\ &= \begin{bmatrix} 1 & 0 & 0 & 0 \\ 0 & 0 & 0 & 1 \\ 0 & 1 & 1 & 0 \end{bmatrix} \begin{Bmatrix} \partial u / \partial x \\ \partial y / \partial y \\ \partial v / \partial x \\ \partial u / \partial y \end{Bmatrix} \end{aligned} \quad (2.24)$$

And we know that:

$$\begin{aligned} \frac{\partial x}{\partial s} &= \begin{bmatrix} \frac{\partial N_1}{\partial s} & \frac{\partial N_2}{\partial s} & \frac{\partial N_3}{\partial s} & \frac{\partial N_4}{\partial s} \end{bmatrix} \begin{Bmatrix} x_1 \\ x_2 \\ x_3 \\ x_4 \end{Bmatrix} \\ &= 1/4[t-1 \quad 1-t \quad 1+t \quad -(1+t)] \begin{Bmatrix} x_1 \\ x_2 \\ x_3 \\ x_4 \end{Bmatrix} \end{aligned} \quad (2.25)$$

$$\begin{aligned} \frac{\partial x}{\partial t} &= \begin{bmatrix} \frac{\partial N_1}{\partial t} & \frac{\partial N_2}{\partial t} & \frac{\partial N_3}{\partial t} & \frac{\partial N_4}{\partial t} \end{bmatrix} \begin{Bmatrix} x_1 \\ x_2 \\ x_3 \\ x_4 \end{Bmatrix} \\ &= 1/4[s-1 \quad -1-s \quad 1+s \quad 1-s] \begin{Bmatrix} x_1 \\ x_2 \\ x_3 \\ x_4 \end{Bmatrix} \end{aligned}$$

$$\begin{aligned} \frac{\partial y}{\partial s} &= \begin{bmatrix} \frac{\partial N_1}{\partial s} & \frac{\partial N_2}{\partial s} & \frac{\partial N_3}{\partial s} & \frac{\partial N_4}{\partial s} \end{bmatrix} \begin{Bmatrix} y_1 \\ y_2 \\ y_3 \\ y_4 \end{Bmatrix} \\ &= 1/4[t-1 \quad 1-t \quad 1+t \quad -(1+t)] \begin{Bmatrix} y_1 \\ y_2 \\ y_3 \\ y_4 \end{Bmatrix} \end{aligned} \quad (2.26)$$

$$\frac{\partial y}{\partial t} = \begin{bmatrix} \frac{\partial N_1}{\partial t} & \frac{\partial N_2}{\partial t} & \frac{\partial N_3}{\partial t} & \frac{\partial N_4}{\partial t} \end{bmatrix} \begin{Bmatrix} y_1 \\ y_2 \\ y_3 \\ y_4 \end{Bmatrix}$$

$$=1/4[s - 1 \quad -1 - s \quad 1 + s \quad 1 - s] \begin{Bmatrix} y_1 \\ y_2 \\ y_3 \\ y_4 \end{Bmatrix}$$

Where the rectangular matrix on the right side is an operator matrix; that is $\partial()/\partial x$ and $\partial()/\partial y$ represent the partial derivatives of any variable we put inside the parentheses.

Evaluating the determinant in the numerators, it will be

$$\begin{aligned} \frac{\partial()}{\partial x} &= \frac{1}{|[J]|} \cdot \left[\frac{\partial y}{\partial t} \cdot \frac{\partial()}{\partial s} - \frac{\partial y}{\partial s} \cdot \frac{\partial()}{\partial t} \right] \\ \frac{\partial()}{\partial y} &= \frac{1}{|[J]|} \cdot \left[\frac{\partial x}{\partial s} \cdot \frac{\partial()}{\partial t} - \frac{\partial x}{\partial t} \cdot \frac{\partial()}{\partial s} \right] \end{aligned} \quad (2.27)$$

Where $[J]$ is the determinant of $[J]$.

We can obtain the strains expressed in terms of the natural coordinates (s,t) as:

$$\begin{Bmatrix} \varepsilon_x \\ \varepsilon_y \\ \gamma_{xy} \end{Bmatrix} = \frac{1}{|[J]|} \begin{bmatrix} \frac{\partial y}{\partial t} \cdot \frac{\partial()}{\partial s} - \frac{\partial y}{\partial s} \cdot \frac{\partial()}{\partial t} & 0 \\ 0 & \frac{\partial x}{\partial s} \cdot \frac{\partial()}{\partial t} - \frac{\partial x}{\partial t} \cdot \frac{\partial()}{\partial s} \\ \frac{\partial x}{\partial s} \cdot \frac{\partial()}{\partial t} - \frac{\partial x}{\partial t} \cdot \frac{\partial()}{\partial s} & \frac{\partial y}{\partial t} \cdot \frac{\partial()}{\partial s} - \frac{\partial y}{\partial s} \cdot \frac{\partial()}{\partial t} \end{bmatrix} \begin{Bmatrix} u \\ v \end{Bmatrix} \quad (2.28)$$

Or in another arrangement:

$$\begin{Bmatrix} \partial u / \partial x \\ \partial u / \partial y \\ \partial v / \partial x \\ \partial v / \partial y \end{Bmatrix} = \frac{1}{|[J]|} \begin{bmatrix} \frac{\partial y}{\partial t} & -\frac{\partial y}{\partial s} & 0 & 0 \\ -\frac{\partial x}{\partial t} & \frac{\partial x}{\partial s} & \frac{\partial y}{\partial t} & -\frac{\partial y}{\partial s} \\ 0 & 0 & -\frac{\partial x}{\partial t} & \frac{\partial x}{\partial s} \\ 0 & 0 & \frac{\partial y}{\partial t} & -\frac{\partial y}{\partial s} \end{bmatrix} \begin{Bmatrix} \partial u / \partial s \\ \partial u / \partial t \\ \partial v / \partial s \\ \partial v / \partial t \end{Bmatrix} \quad (2.29)$$

Strain will be:

$$\begin{Bmatrix} \varepsilon_x \\ \varepsilon_y \\ \gamma_{xy} \end{Bmatrix} = \frac{1}{|J|} \begin{bmatrix} 1 & 0 & 0 & 0 \\ 0 & 0 & 0 & 1 \\ 0 & 1 & 1 & 0 \end{bmatrix} \begin{bmatrix} \frac{\partial y}{\partial t} & -\frac{\partial y}{\partial s} & 0 & 0 \\ \frac{\partial x}{\partial t} & \frac{\partial x}{\partial s} & \frac{\partial y}{\partial t} & -\frac{\partial y}{\partial s} \\ 0 & 0 & -\frac{\partial x}{\partial t} & \frac{\partial x}{\partial s} \\ 0 & 0 & -\frac{\partial y}{\partial t} & \frac{\partial y}{\partial s} \end{bmatrix} \begin{Bmatrix} \frac{\partial u}{\partial s} \\ \frac{\partial u}{\partial t} \\ \frac{\partial v}{\partial s} \\ \frac{\partial v}{\partial t} \end{Bmatrix} \quad (2.30)$$

$$= [A] \begin{Bmatrix} \frac{\partial u}{\partial s} \\ \frac{\partial u}{\partial t} \\ \frac{\partial v}{\partial s} \\ \frac{\partial v}{\partial t} \end{Bmatrix}$$

But:

$$\begin{Bmatrix} \frac{\partial u}{\partial s} \\ \frac{\partial u}{\partial t} \\ \frac{\partial v}{\partial s} \\ \frac{\partial v}{\partial t} \end{Bmatrix} = \frac{1}{4} \begin{bmatrix} t-1 & 0 & 1-t & 0 & 1+t & 0 & -(t+1) & 0 \\ s-1 & 0 & -(s+1) & 0 & 1+s & 0 & 1-s & 0 \\ 0 & t-1 & 0 & 1-t & 0 & 1+t & 0 & -(t+1) \\ 0 & s-1 & 0 & -(s+1) & 0 & 1+s & 0 & 1-s \end{bmatrix} \times \begin{Bmatrix} u_1 \\ v_1 \\ u_2 \\ v_2 \\ u_3 \\ v_3 \\ u_4 \\ v_4 \end{Bmatrix} \quad (2.31)$$

$$= [G]\{q\}$$

from this step we get:

$$[B] = [A][G] \quad (2.32)$$

So strain:

$$\begin{Bmatrix} \varepsilon_x \\ \varepsilon_y \\ \gamma_{xy} \end{Bmatrix} = [A][G]\{q\} = [B]\{q\} \quad (2.33)$$

And because [K] is:

$$[K] = h \iint_A [B]^T [C][B]dA \quad (2.34)$$

In (s,t) form will be:

$$[K] = h \iint_{-1}^1 [B]^T [D][B]|J|ds. dt \quad (2.35)$$

[D] represents the stress/strain matrix (or constitutive matrix), in plane stress will be:

$$[D] = \begin{bmatrix} E/(1-\vartheta^2) & \vartheta E/(1-\vartheta^2) & 0 \\ \vartheta E/(1-\vartheta^2) & E/(1-\vartheta^2) & 0 \\ 0 & 0 & E/2(1+\vartheta) \end{bmatrix} \quad (2.36)$$

[D] in plane strain is:

$$[D] = \begin{bmatrix} E(1-\vartheta)/(1+\vartheta)(1-2\vartheta) & E\vartheta/(1+\vartheta)(1-2\vartheta) & 0 \\ E\vartheta/(1+\vartheta)(1-2\vartheta) & E(1-\vartheta)/(1+\vartheta)(1-2\vartheta) & 0 \\ 0 & 0 & E/2(1+\vartheta) \end{bmatrix} \quad (2.37)$$

Using Gauss interpolation we will have [K] in the form:

$$[K] = h \sum_{i=1}^n \sum_{j=1}^n w_i w_j ([B]^T [D][B]|J|)_{ij} ds. dt \quad (2.38)$$

2.2.4 Stress / Strain Matrix (or Constitutive Matrix)

For isotropic materials and assuming plane stress so :

$$\sigma_z = \tau_{xz} = \tau_{yz} = 0$$

And (2.39)

$$\gamma_{xz} = \gamma_{yz} = 0$$

Yields

$$\{\sigma\} = [D]\{\varepsilon\} \quad (2.40)$$

Where

$$[D] = \left(\frac{E}{1-\vartheta^2}\right) \begin{bmatrix} 1 & \vartheta & 0 \\ \vartheta & 1 & 0 \\ 0 & 0 & (1-\vartheta)/2 \end{bmatrix} \quad (2.41)$$

[D] represents the stress/strain matrix(or constitutive matrix), E Modulus of elasticity and ϑ is poisson' s ratio.

The strain in plane stress will be:

$$\{\varepsilon\} = [C]\{\sigma\} \quad (2.42)$$

Or

$$\begin{Bmatrix} \varepsilon_x \\ \varepsilon_y \\ \gamma_{xy} \end{Bmatrix} = \left(\frac{1}{E}\right) \begin{bmatrix} 1 & -\vartheta & 0 \\ -\vartheta & 1 & 0 \\ 0 & 0 & 2(1+\vartheta) \end{bmatrix} \begin{Bmatrix} \sigma_x \\ \sigma_y \\ \sigma_{xy} \end{Bmatrix} \quad (2.43)$$

Where

$$[C]^{-1}=[D] \quad (2.44)$$

$$\varepsilon_y = \left(\frac{1}{E}\right)(-\vartheta)(\sigma_x + \sigma_y) \quad (2.45)$$

2.2.5 Evaluate a Line Distributed Load

To evaluate a line distributed load, the face of element which is subjected to this load must be determined first. Retaining back to Figure 2.3 and depending on the number of the face Jacobian matrix [J] will be [20]:

- At the first face, between node 1, and node 2, where $t=-1$

$$J^1 = \left[\left(\frac{\partial x}{\partial s} \right)^2 + \left(\frac{\partial y}{\partial s} \right)^2 \right]^{1/2} \quad (2.46)$$

- At the second face, between node 2, and node 3, where $s=1$

$$J^2 = \left[\left(\frac{\partial x}{\partial t} \right)^2 + \left(\frac{\partial y}{\partial t} \right)^2 \right]^{1/2} \quad (2.47)$$

- At the third face, between node 3, and node 4, where $t=1$

$$J^3 = \left[\left(\frac{\partial x}{\partial s} \right)^2 + \left(\frac{\partial y}{\partial s} \right)^2 \right]^{1/2} \quad (2.48)$$

- At the fourth face, between node 4, and node 1, where $s=-1$

$$J^4 = \left[\left(\frac{\partial x}{\partial t} \right)^2 + \left(\frac{\partial y}{\partial t} \right)^2 \right]^{1/2} \quad (2.49)$$

Where the local load (f) of this node will be:

$$f = \begin{bmatrix} N_1 \\ N_2 \end{bmatrix} [1 - s/l \quad s/l] \times J^{(i)} \times \begin{bmatrix} tx \\ ty \end{bmatrix} \quad (2.50)$$

N_1, N_2 are the discretization of facing load, l is the length of that face, and tx, ty are the traction load on $x-, y-$ direction at the face.

2.2.6 Functionally Graded Material (FGM)

Material properties in Functionally Graded Material (FGM) are blended by means of the following equation [14], [21].

$$P_e = P_1 V_1 + P_2 V_2 \quad (2.51)$$

Where P_e is the effective property; P_1 and P_2 are the material property for first and second material, respectively. This property includes Young's modulus E and Poisson's ratio ν . The notations V_1 and V_2 are the volume fractions of these materials.

In this FE-code it is considered that volume fractions change with a continuous function along the main direction of the material (X-direction).

$$V_1 = ((x-x_1)/L)^n \quad (2.52)$$

And

$$V_2 = 1 - V_1 \quad (2.53)$$

Where L is the depth of continuum shown in Figure 2.6, n is a material index which indicates the material variation profile along the thickness of FGM. For examples, $n = 0$ corresponds to an isotropic homogeneous of material 1 and $n = \infty$ corresponds to an isotropic homogeneous material 2.

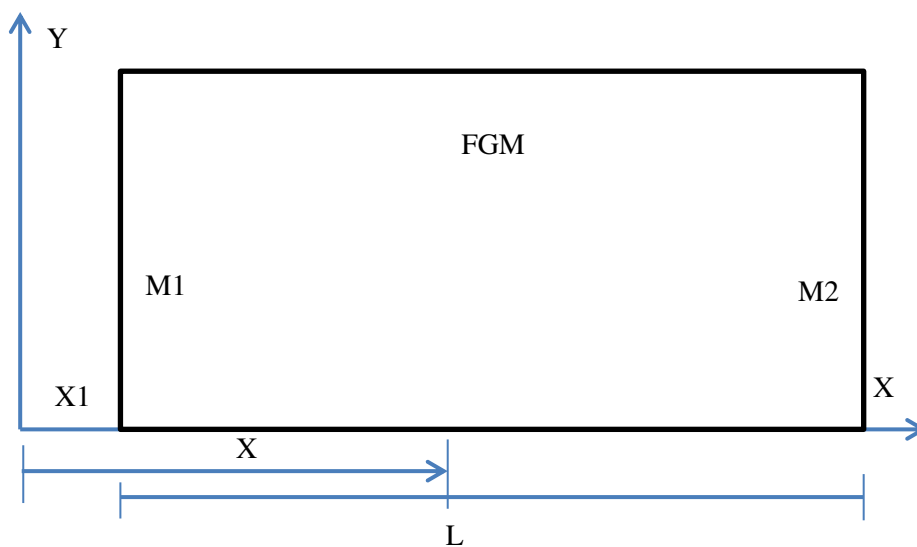


Figure 2.6 The FGM model in this study

PROGRAMMING THE FE-CODE

3.1 The Code Main Frame

MATLAB language is used for developing the developed finite element code (FE-code). This FE-code follows main steps which are given in chart shown in Figure (3.1). It applies distributed load, concentrated load, and includes Functionally Graded Material (FGM), and non-graded material.

3.1.1 Input Data

In the beginning of any numerical program, a definition data of the structural problem must be defined. The geometry, mechanical property, boundary condition, and load are defined in matrix formula.

The geometry definition is done by:

- Defining the (x,y) for every node of the body.
- Determining the nodes of every element.

And after that, boundary conditions must be announced to know the degree of freedom of the problem. The mechanical property is given for every material of the problem. It consists of the Modulus of elasticity E, Poisson's ratio ν . Also, the loading type, magnitude, and location are defined. Finally, the weight of Gauss quadrature is announced.

3.1.2 Compute Local Stiffness Matrix and Local Load Vector for Elements

This part of the program evaluates the stiffness matrix for each element Figure 3.2. It computes at each GAUSS points (s, t):

- The shape functions N and their derivatives $\frac{\partial N}{\partial s}, \frac{\partial N}{\partial t}$ [22].
- Jacobian matrix [J].

- Element matrix [B].
- Material matrix [D], for non-FGM or FGM.
- Local stiffness matrix [k].
- Local vector load [f]. A subroutine program is created to evaluate line distributed load.

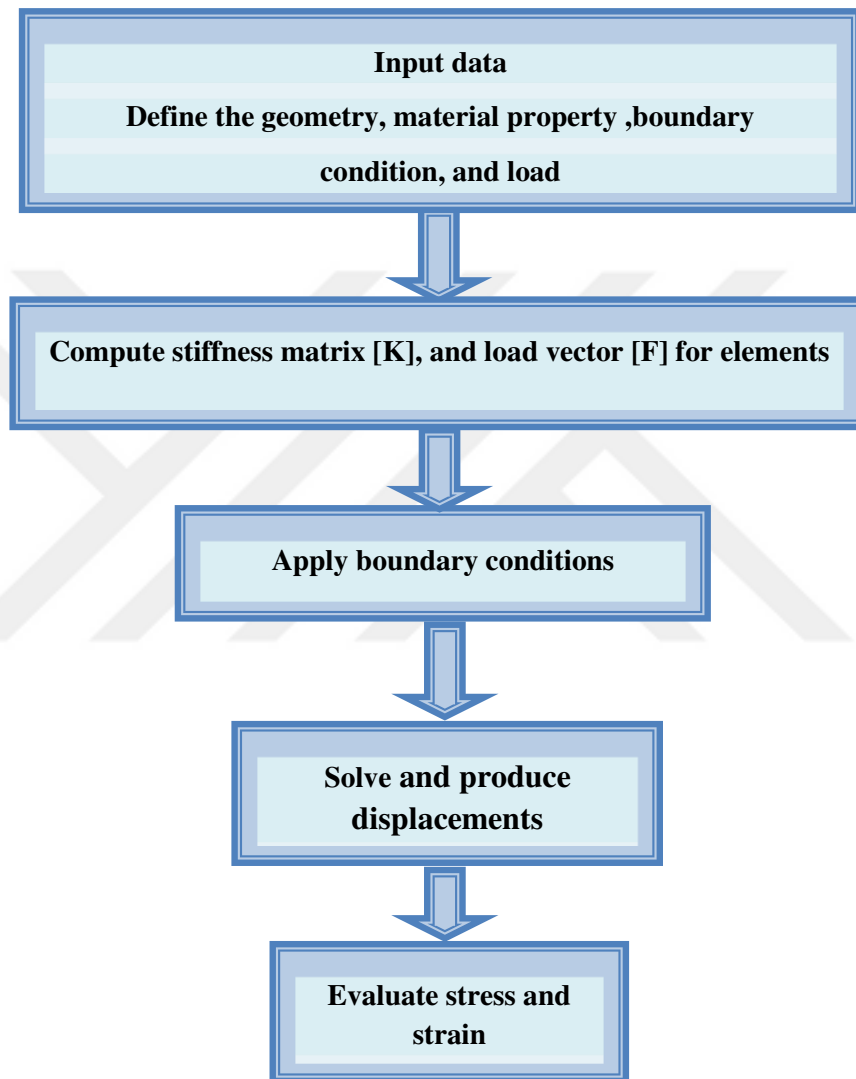


Figure 3.1 Flowchart of the FE-code.

The FE-code contains many subroutine programs (functions) to control every problem and gives the developer more efficiency to use it.

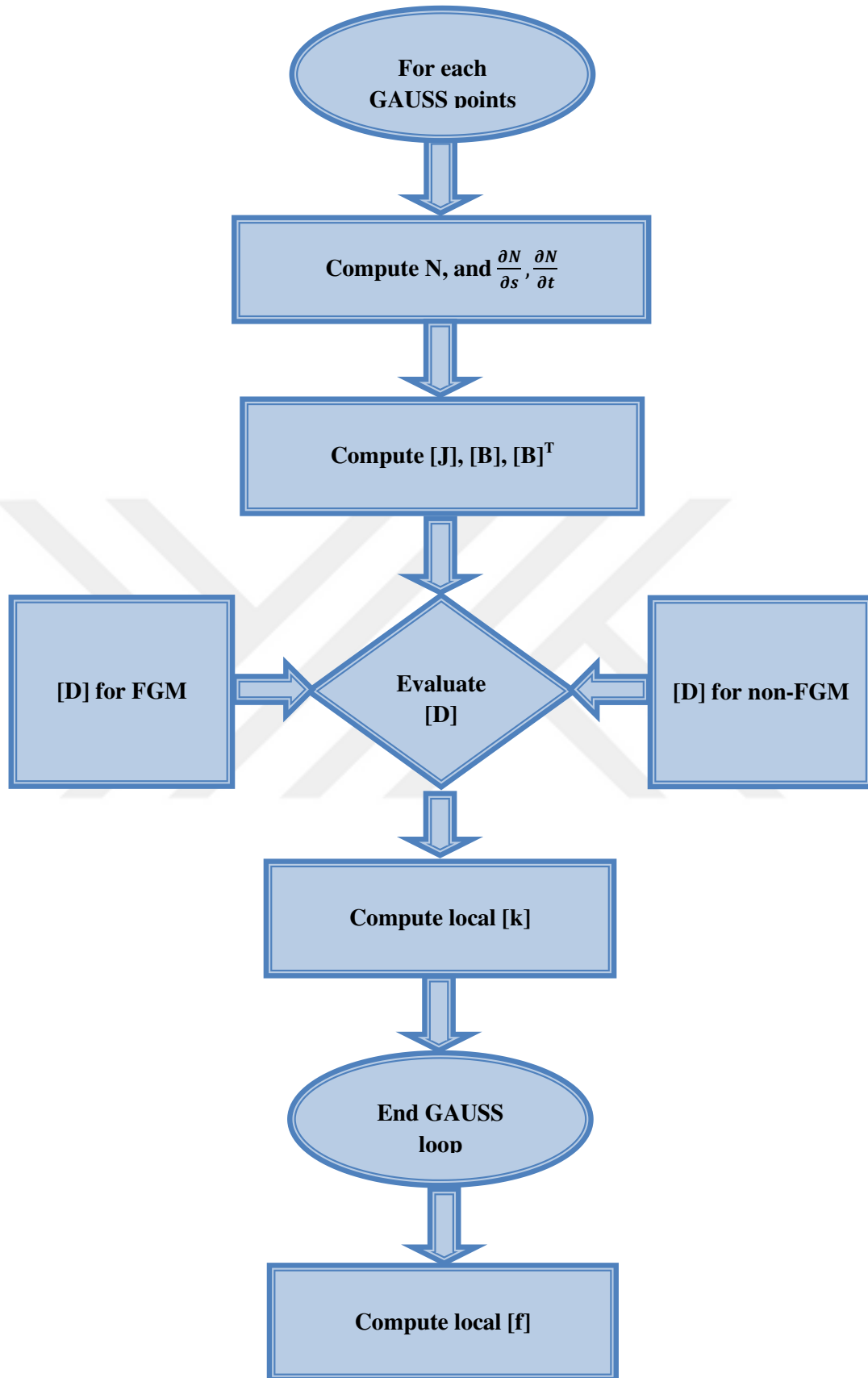


Figure 3.2 Flowchart of computing local stiffness matrix [k], and local load vector [f] for elements

As seen in Figure 3.2, this part of code deals with the calculating of local stiffness matrix $[k]$, and local load vector $[f]$ for every elements of continuum.

3.1.3 Global Stiffness Matrix $[K]$, and Global Load Vector $[F]$

Here a programming steps are done to distribute the local $[k]$, $[f]$ into their global locations in global $[K]$, $[F]$. After that assembling, the boundary conditions are added to the global $[K]$, $[F]$.

Finally, program solves and produces displacements and then evaluates stress and strain.

3.2 Important Subroutine

3.2.1 Line Distributed Load

In this loading case, a special subroutine program is built to compute load at every node subjected to traction load.

Figure 3.3 shows a flowchart of compute local load vector $[f]$ for elements subjected to traction load.

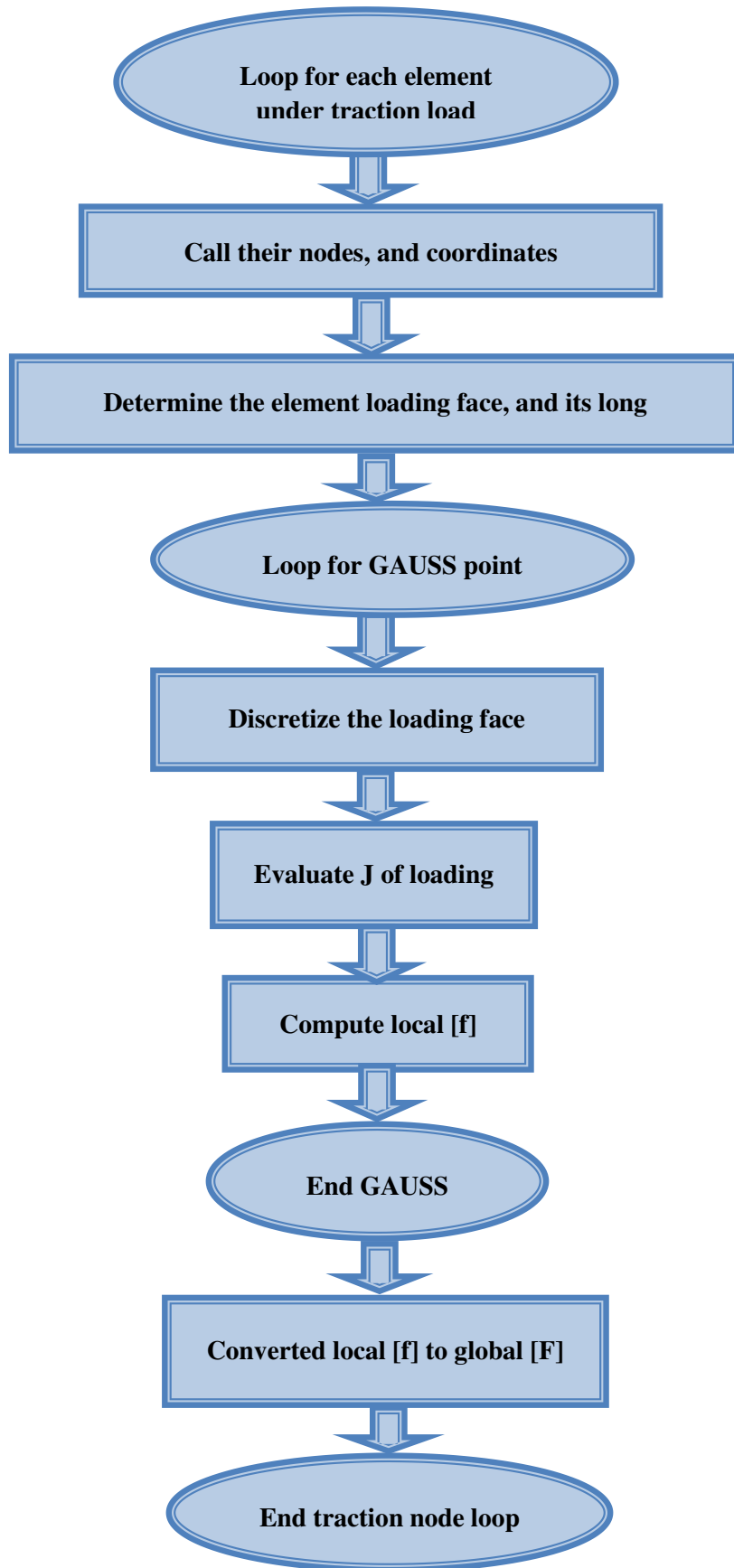


Figure 3.3 Flowchart of computing global load vector [F] from line load.

This part of code deals with line load. It calls the nodes which under the line load and by determining the face of loading for every node it calculates the local load vector [f].

3.2.2 Material Matrix [D] for FGM

This matrix depends on material type. For FGM, [D] is computed as shown in the flowchart of Figure 3.4.

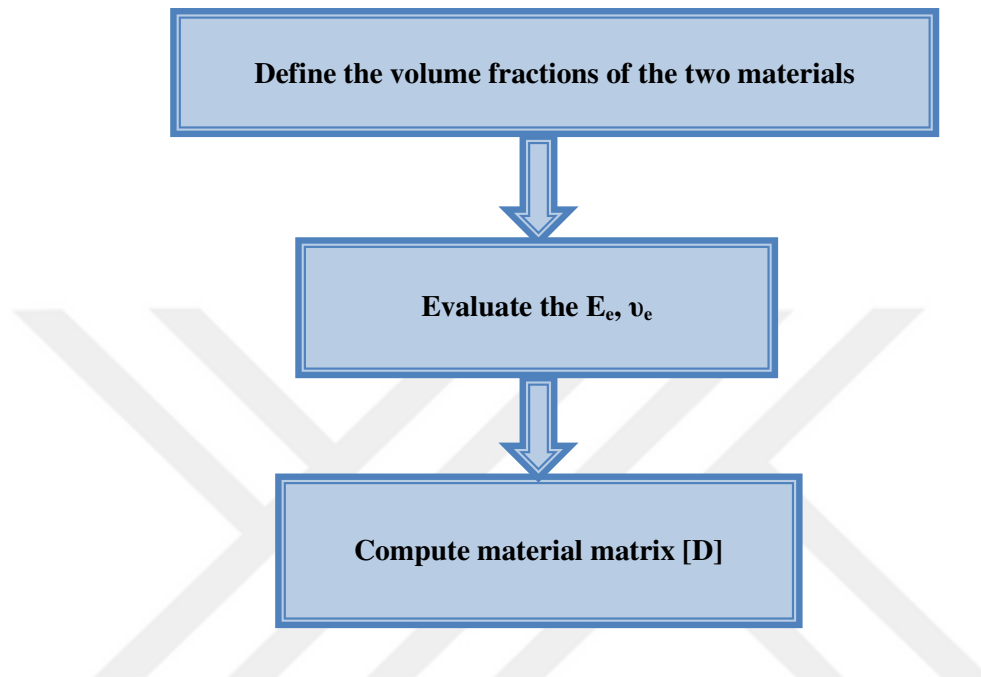


Figure 3.4 Computing material matrix [D]for FGM

Here, material matrix [D] is calculated after defining of material index which indicates the material variation profile along the thickness of FGM.

NUMERICAL PROBLEMS

Three groups of plane stress problems will be solved within the FE-code. The first group includes two problems of patch tests, which are considered for verification of the FE-code with their results. Exact and numerical results about patch tests are given in literature.

The second group covers two problems. One is about deformed beam with concentrated load and the other is a retaining wall with a triangular distributed pressure load. This group will be solved also by the ABAQUS program to make results comparison.

The third group deals with main structural problems of this study, which is related with Functionally Graded Material (FGM). First problem of this group is a retaining wall and the second is an embedded water tank.

Therefore the groups could be classified into:

- Patch test group.
- ABAQUS program group.
- Functionally Graded Material (FGM) group.

4.1 Patch Test Group

These problems are considered as a plane stress problems. Here, exact and numerical results for specific points are given in literature [23].

4.1.1 First Patch Test

In this problem a linear material is involved with a modulus of elasticity, E , of 1500 unit; Poisson ratio, ν , of 0.25 unit; thickness, h , of 1 unit. Its mesh structure is demonstrated in Figure 4.1. The deformed shape is shown in Figure 4.2. Exact and numerical results for displacements of point A and stress of point B seen in Figure 4.2 are given in literature [23].

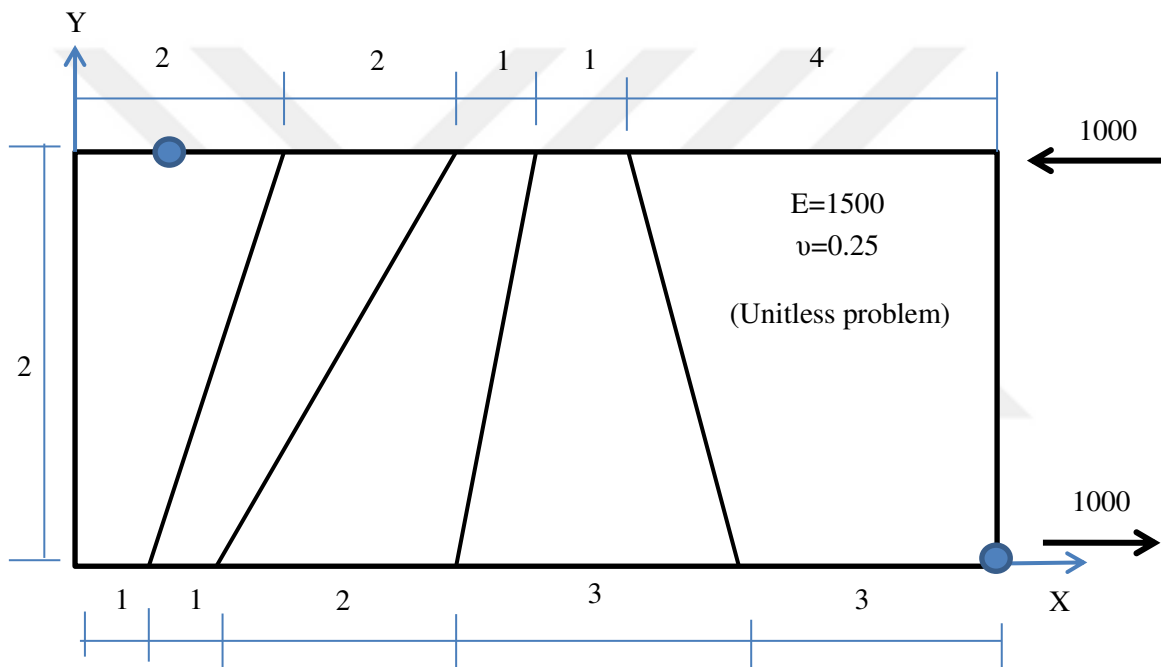


Figure 4.1 Geometry, load pattern, and mesh of Patch problem [23].

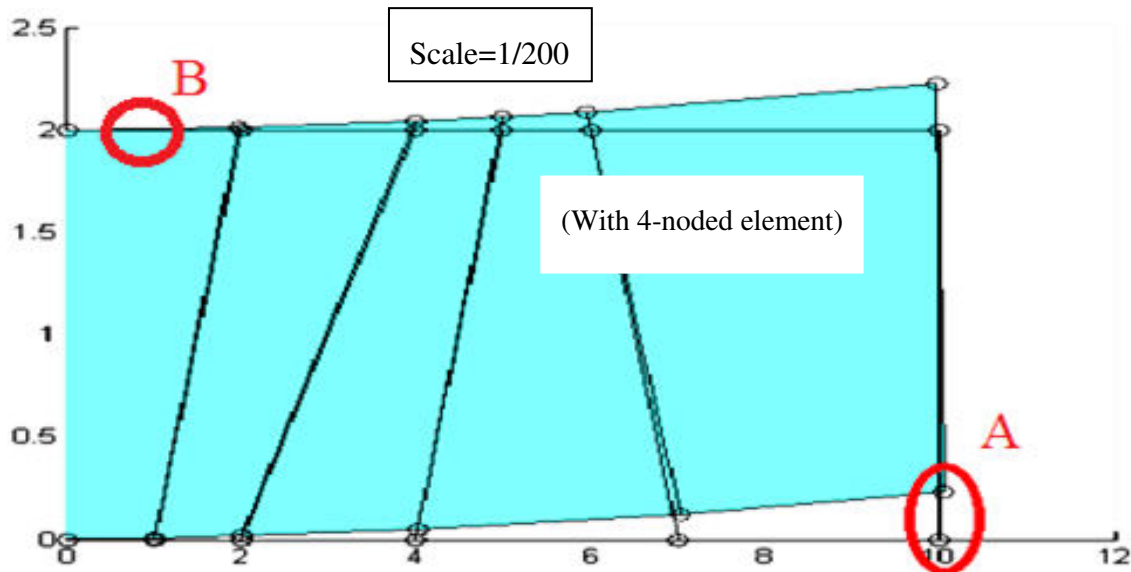


Figure 4.2 The deformed shape of Patch problem.

Comparisons of displacement and stress results for 4-noded; 8-noded; 17-noded elements with the exact results are given in Table 4.1 and Table 4.2, respectively. Moreover, numerical results for 4-noded element given in literature are included in Table 4.1 and Table 4.2.

Table 4.1 Comparisons of displacement results for 4-noded; 8-noded; 17-noded elements with the results given in literature [23].

Displacement	The exact value [23]	Numerical value in literature [23]	FE-code	Element type	Number of Gauss points
Displacement of point A in direction of Y	100.00	45.70	45.65	4-noded element	2
			99.70	8-noded element	3
			99.78	17-noded element	5

Table 4.2 Comparisons of stress results in horizontal direction for 4-noded; 8-noded; 17-noded elements with the results given in literature [23].

Stress	The exact value [23]	Numerical value in literature [23]	FE-code	Element type	Number of Gauss points
Stress of point B in direction of X	-3000.00	-1761.00	-1761.63	4-noded element	2
			-2983.46	8-noded element	3
			-3122.55	17-noded element	5

As seen in Table 4.1, approximately 46% of the exact result and approximately 100% of the numerical result are reached by 4-noded element in displacement field. The poor performance is expected because of no improvement in this element, 8-noded and 17-noded elements give approximately 99% of the exact result. This achievement results from interpolation qualities of the elements.

As seen in Table 4.2, 4-noded element achieves approximately 58% of the exact result and approximately 100% of the numerical result in stress field. While 8-noded gives approximately 100% of the exact result, 17-noded element reaches stress result a little greater than 100% of the exact result.

4.1.2 Second Patch Test

This problem was the same geometry and material property with previous patch test problem, but different load pattern as demonstrated in Figure 4.3. The deformed shape is shown in Figure 4.4. Exact and numerical results for displacement of point A and stress of point B seen in Figure 4.4 are given in literature [23].

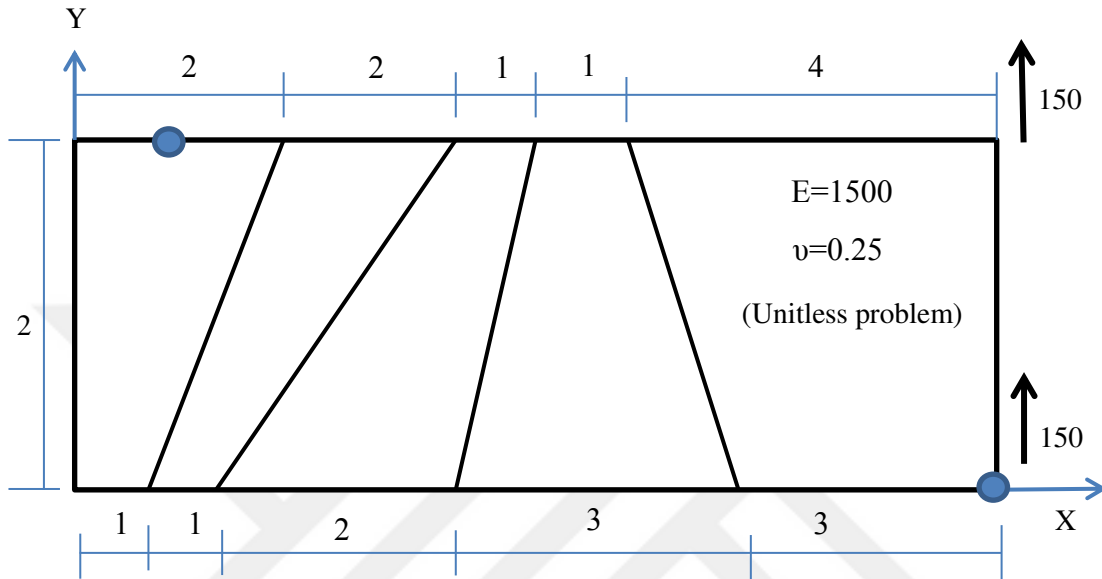


Figure 4.3 Geometry, load pattern, and mesh of Patch problem [23].

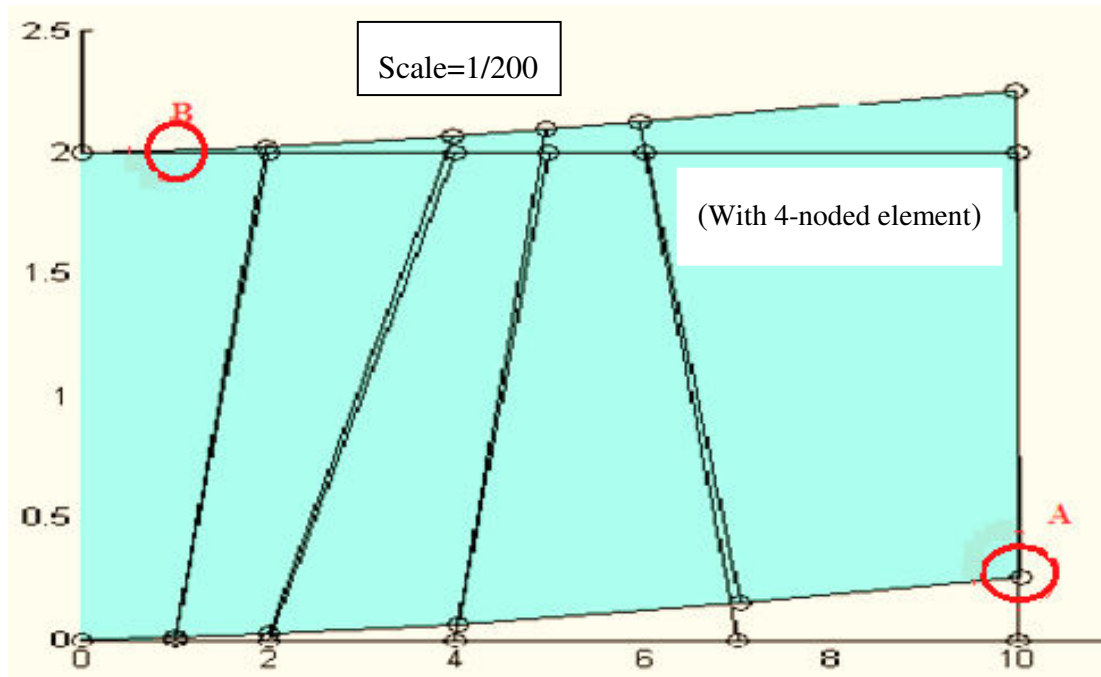


Figure 4.4 The deformed shape of Patch problem.

Comparisons of displacement and stress results for 4-noded; 8-noded; 17-noded elements with the exact results are given in Table 4.3 and Table 4.4, respectively. Moreover, numerical results for 4-noded element given in literature are included in Table 4.3 and Table 4.4.

Table 4.3 Comparisons of displacement results for 4-noded; 8-noded; 17-noded elements with the results given in literature [23].

Displacement	The exact value [23]	Numerical value in literature [23]	FE-code	Element type	Number of gauss points
Displacement of point A in direction of Y	102.60	50.70	50.96	4-noded element	2
			101.76	8-noded element	3
			102.25	17-noded element	5

Table 4.4 Comparisons of stress results in horizontal direction for 4-noded; 8-noded; 17-noded elements with results given in literature [23].

Stress	The exact value [23]	Numerical value in literature [23]	FE-code	Element type	Number of gauss points
Stress of point B in direction of X	-4050.00	-2448.00	-2447.82	4-noded element	2
			-4060.21	8-noded element	3
			-4266.38	17-noded element	5

As seen in Table 4.3, approximately 49% of the exact result and approximately 98% of the numerical result are reached by 4-noded element in displacement field. 8-noded and 17-noded elements give approximately 99% and 100% of the exact result, respectively.

As seen in Table 4.4, 4-noded element fulfils approximately 60% of the exact result and approximately 100% of the numerical result in stress field. While 8-noded element gives approximately 100% of the exact result, 17-noded element carries out stress result a little greater than 100% of the exact result.

In both of the patch tests, 4-noded, 8-noded, and 17-noded elements make widely known similar behavior in displacement field and stress field, respectively.



4.2 ABAQUS Program Group

These two problems will be solved by the ABAQUS program also to make results comparison.

4.2.1 A Retaining Wall

A concrete retaining wall is considered as a plane stress problem and it is supposed to a pressure. Modulus of elasticity of concrete, E , is 2.0×10^7 kN/m²; Poisson ratio, ν , is 0.3; thickness, h , is 1m. Load pattern acts as a triangular distributed load of $P = \gamma_w \cdot h$ ($\gamma_w = 1.0$ kN/m³) behind the retaining wall. Moreover, mesh structure and dimensions are seen in Figure 4.5.

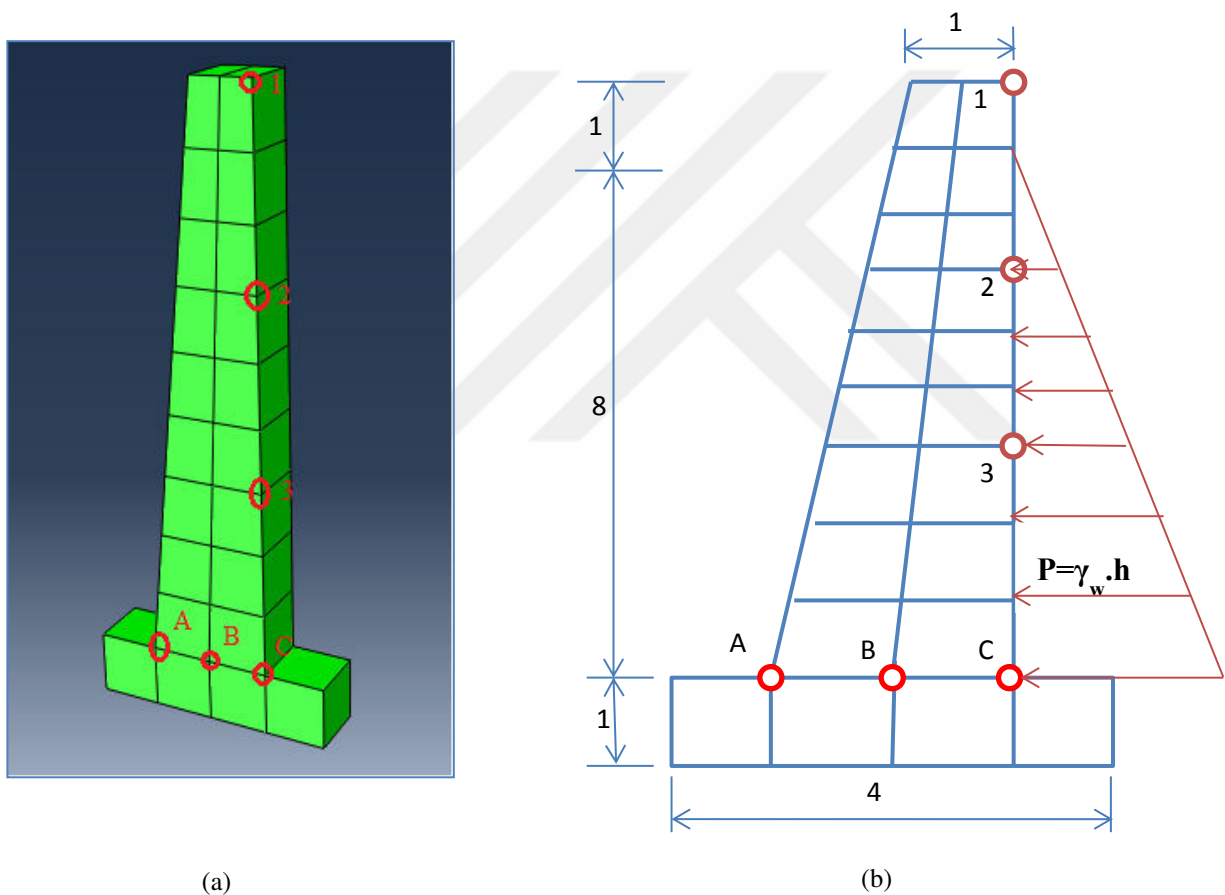
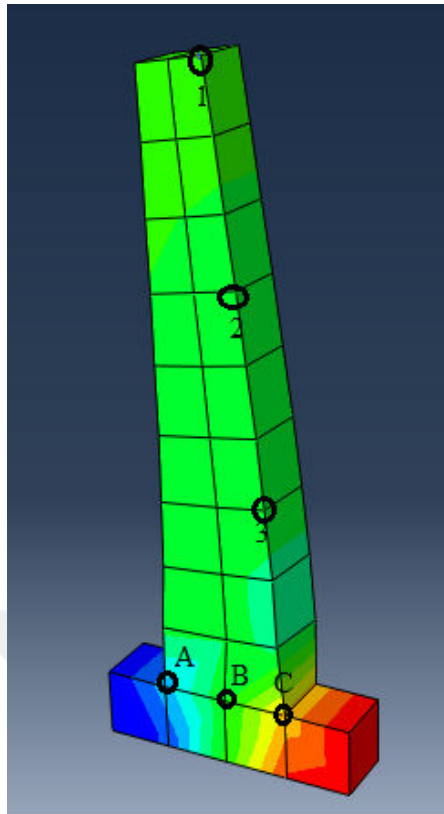
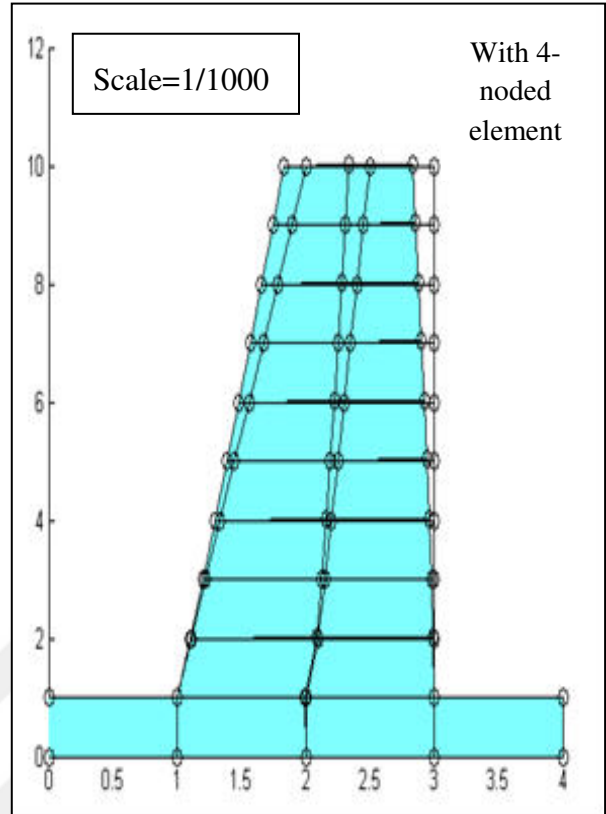


Figure 4.5 a) Mesh structure of retaining wall within ABAQUS, and b) Mesh, load pattern, and geometry of the FE-code (all dimensions in meters).

When using 4-noded element, the deformed shape is shown in Figure 4.6. Here the comparison of results within the ABAQUS and the FE-code is given in Table 4.5. Displacement results are given for point 1, 2, and 3 and stress results are observed for point A, B, and C, which are seen in Figure 4.6 b.



(a)



(b)

Figure 4.6 The deformed shapes for the retaining wall within a) ABAQUS and b) The FE-code.

Table 4.5 Comparison of results of the FE-code for retaining wall with non- FGM and ABAQUS.

Element type	Number of gauss points	Displacement in horizontal direction, m ($\times 10^{-5}$)			Stress in horizontal direction, kN/m^2					
		1	2	3	A		B		C	
					Element nodes	Gauss points	Element nodes	Gauss points	Element nodes	Gauss points
4-noded	2	-17.00	-10.00	-4.00	-29.90	-22.60	-0.80	-1.20	30.70	22.40
8-noded	3	-19.00	-12.00	-4.00	-42.80	-23.40	1.00	-0.50	41.50	21.60

Table 4.5 Comparison of results of the FE-code for retaining wall with non- FGM and ABAQUS (cont'd)

Element type	Number of gauss points	Displacement in horizontal direction, m ($\times 10^{-5}$)			Stress in horizontal direction, kN/m ²					
		1	2	3	A		B		C	
					Element nodes	Gauss points	Element nodes	Gauss points	Element nodes	Gauss points
17-noded	5	-20.00	-12.00	-5.00	-67.50	-23.10	-1.50	-0.70	67.50	21.20
ABAQUS	-----	-22.00	-13.00	-6.00	-17.20		-1.30		15.00	

As seen in Table 4.5, 70-80 % of displacements in ABAQUS are reached by 4-noded element, while 8-noded and 17-noded elements give 80-90 % of displacement in ABAQUS. Moreover, Table 4.5 shows that stresses in horizontal direction keep developing as expected on the element nodes.

Here, stresses are evaluated in just on the element nodes. This evaluation approach of stress results in the stress concentration in point A and point C where geometry of the problem dramatically changes. However, when gauss points instead of the element nodes in the evaluation of stress are used, the stress results are getting converged as in Table 4.5.

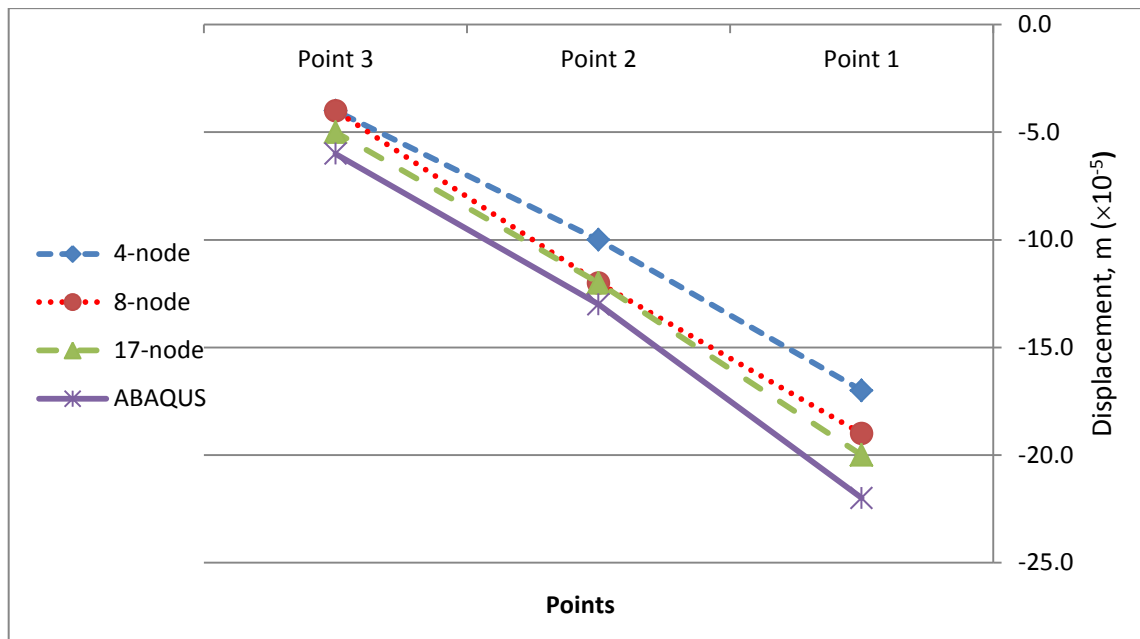


Figure 4.7 Displacement results for the retaining wall.

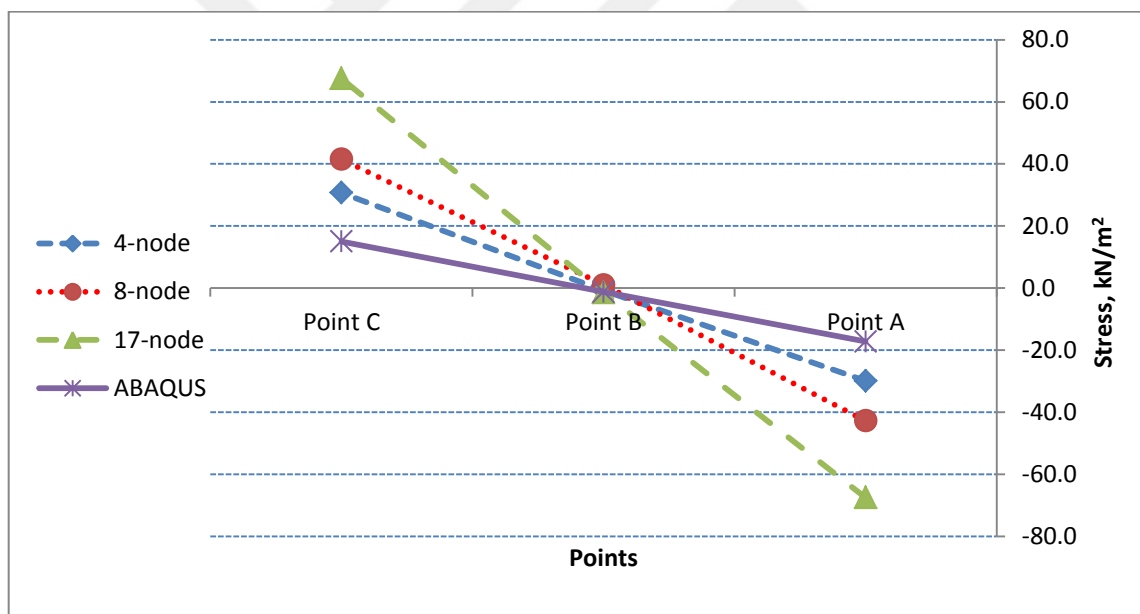


Figure 4.8 Stress results in horizontal direction for the retaining wall.

As seen in Figure 4.7 and Figure 4.8, a higher order element effect on the results of displacements and stresses is clearly seen, respectively. Displacement results of 8-, 17-noded element are so similar, and they have a similar tendency within ABAQUS results in Figure 4.7. Slope of stresses from point A to point C keeps increasing while the number of nodes within quadrilateral elements increases in the FE-code. By the way, the slope of stress for ABAQUS seems less than the slopes for FE-code.

4.2.2 A Deformed Steel Beam

A deformed steel beam is considered as a plane stress problem. Its length, $L=400$ cm. Modulus of elasticity of steel, E , is 210 GPa; Poisson ratio, ν , is 0.03; with the dimensions appears in Figure 4.9, it is fixed at 1 m in each side where there is a fixed connection with a column, and it is forced by two concentrated load of 1.5×10^4 kg inclined with 74.36° at the points which appear in Figure 4.10, to get it back to its original shape (move the upper flange 2.0 cm in horizontal direction).

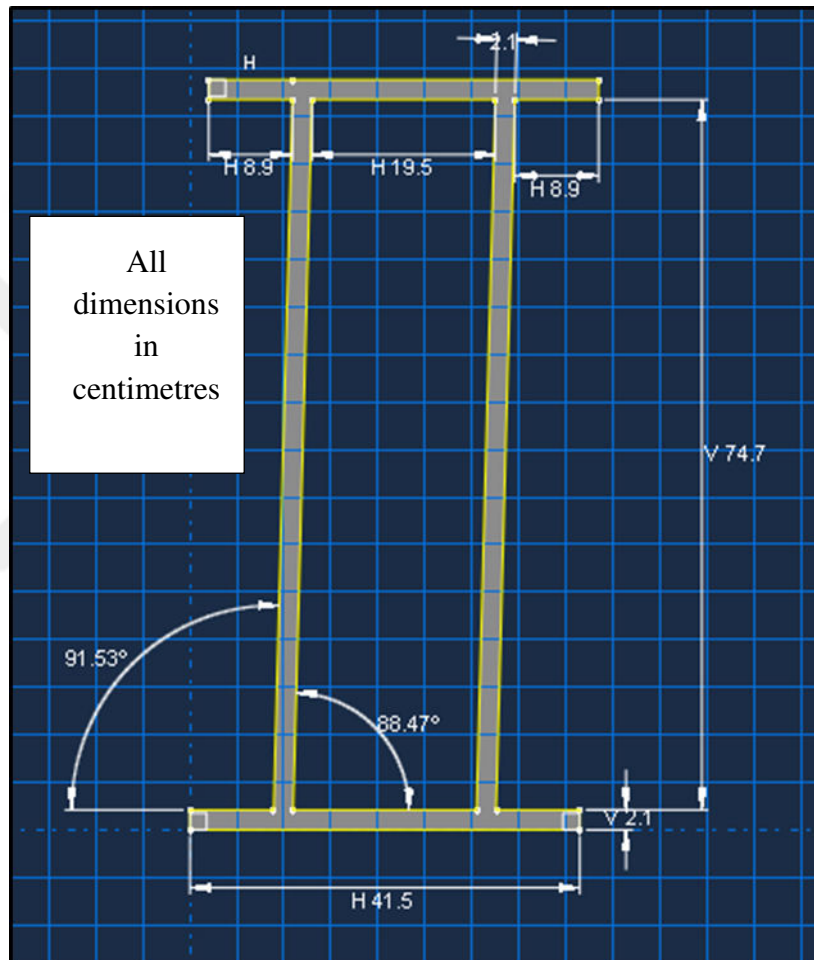


Figure 4.9 The deformed steel beam section.

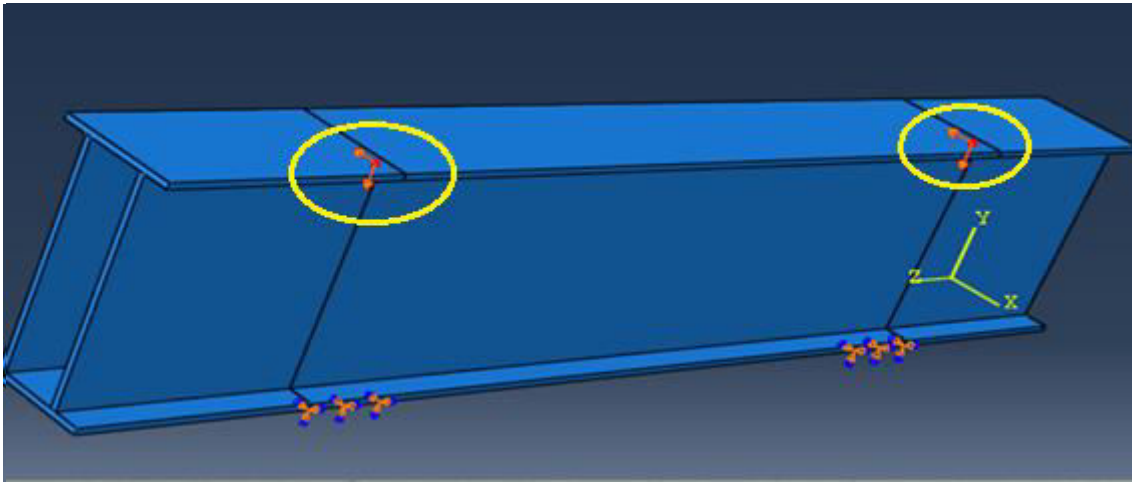


Figure 4.10 The supporting and loading points of the deformed steel beam.

The deformed shape of beam is shown within ABAQUS and with 4-noded element in the FE-code.

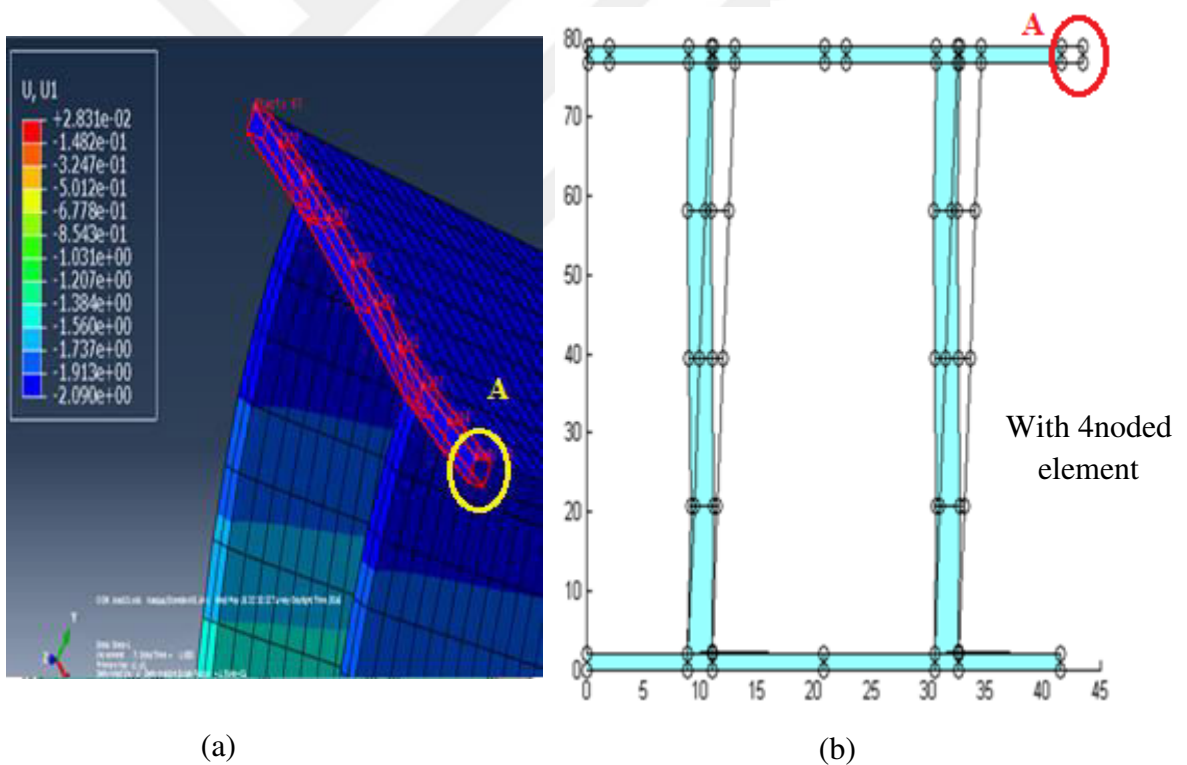


Figure 4.11 The deformed shapes for the beam within a) ABAQUS and b) The FE-code.

ABAQUS gives -2.09 cm of displacement, while the FE-code with 4-noded element achieves -1.908 cm of displacement.

This deformed beam has been examined in Laboratory of Structure Design in Civil Engineering Department in Yıldız Technical University. A 2.0 cm of displacement at the level of upper flange in horizontal direction is measured to fix the beam. Therefore, the 4-noded element achieves with 4.6% difference while ABAQUS is got with 4.5% difference.



4.3 Functionally Graded Material (FGM) group.

The main problems of this study which deal with FGM. In the analysis of these structural problems, it is assumed that wall material is FGM just in horizontal direction.

4.3.1 A Retaining Wall with FGM

A retaining wall material of which is Functionally Graded Material (stone and mortar in the upper part with concrete base) is considered as a plane stress problem. It is supposed to soil pressure and is shown in Figure 4.12. Its thickness, h is 1m. A triangular distributed load of $P=\gamma_s \cdot h$ ($\gamma_s = 1.8 \text{ kN/m}^3$) acts behind the retaining wall, mesh structure and the dimension are given in Figure 4.13.

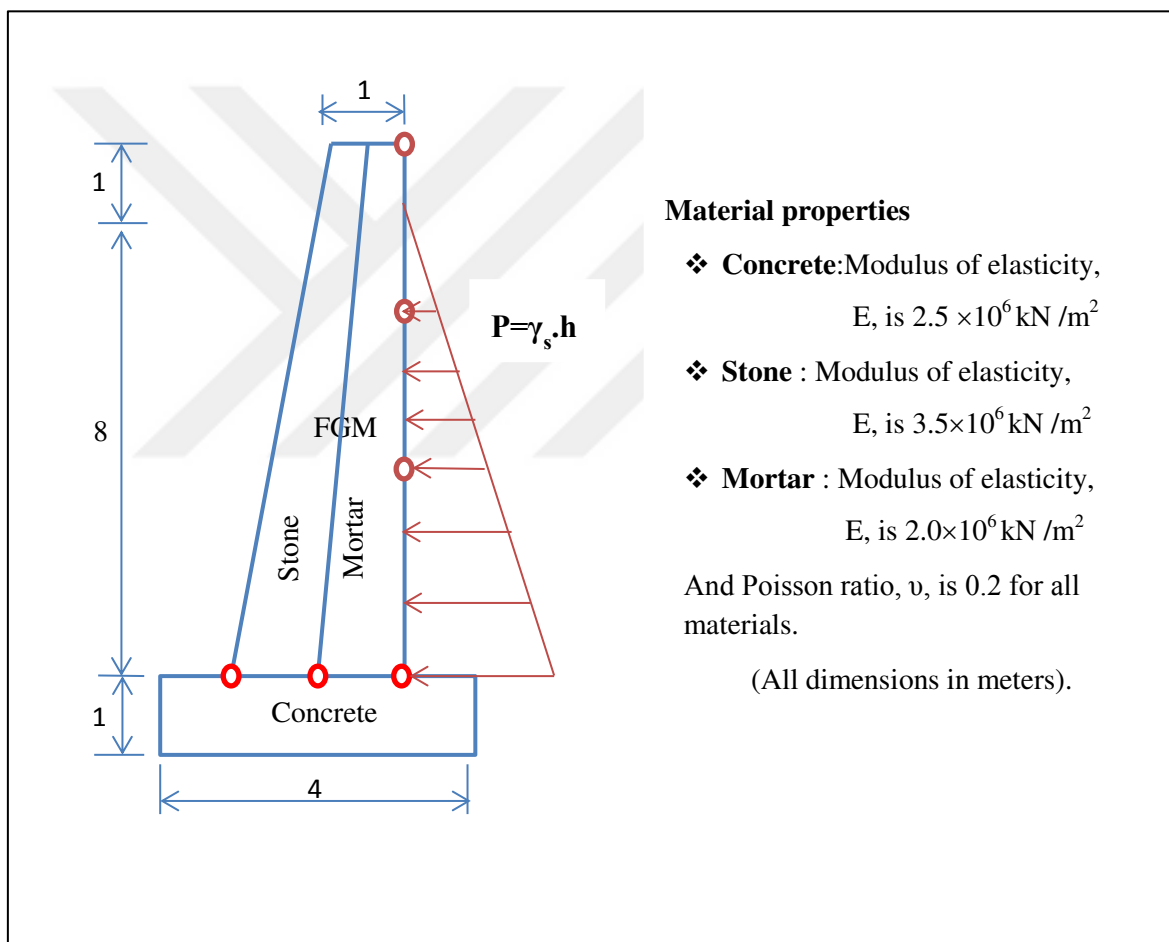


Figure 4.12 Load pattern, geometry, and material property of the retaining wall with FGM.

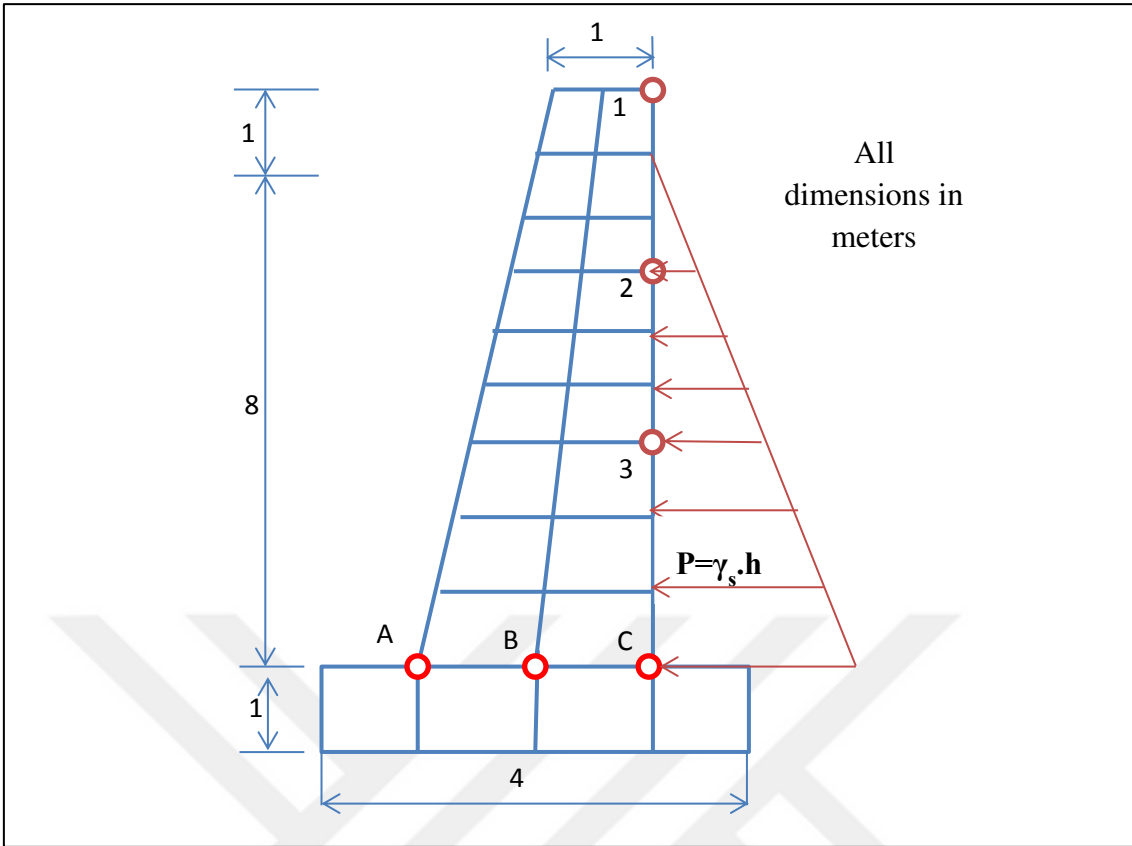


Figure 4.13 Mesh structure of the retaining wall with FGM.

The results of selected points shown in Figure 4.13 are given in the Table 4.6 and the deformed shape is shown in Figure 4.14.

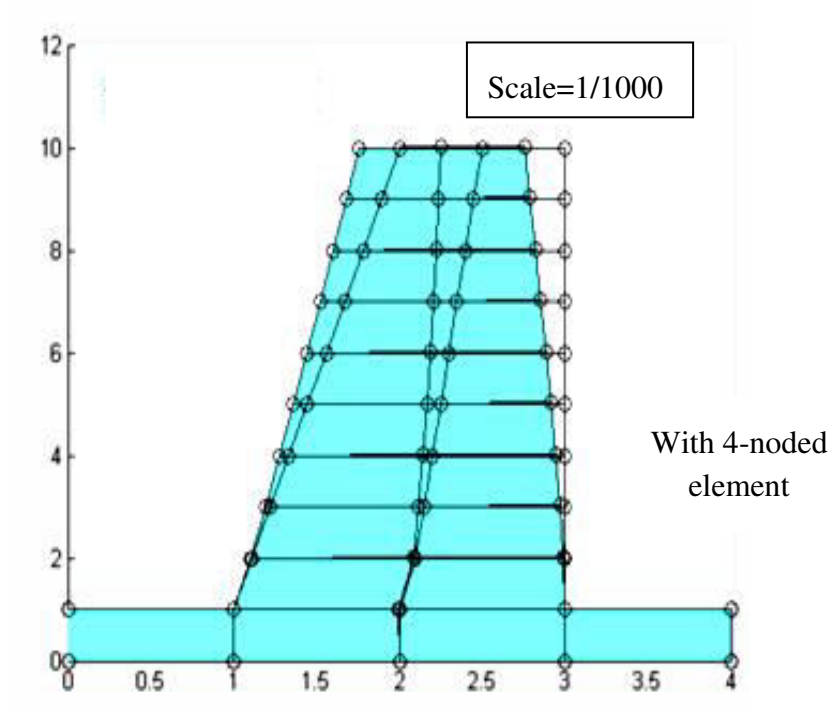


Figure 4.14 The deformed shape of retaining wall with FGM for 4-noded element

Table 4.6 Displacement and stress results in horizontal direction of retaining wall with FGM.

Element type	Number of gauss points	Displacement in horizontal direction, m ($\times 10^{-5}$)			Stress in horizontal direction, kN/m ²					
		1	2	3	A		B		C	
					Element nodes	Gauss points	Element nodes	Gauss points	Element nodes	Gauss points
4-noded	2	-24.00	-15.00	-6.00	-46.23	-35.07	-0.48	-1.69	47.79	32.72
8-node	3	-28.00	-17.00	-6.00	-75.11	-40.74	2.21	-0.17	74.17	35.64
17-noded	5	-29.00	-17.00	-7.00	-121.29	-40.78	0.62	-0.59	118.94	35.97

As appears in Table 4.6, results of displacements are seen more close as the number of nodes within quadrilateral elements increases. However, results of stresses keep on developing when the number of nodes within quadrilateral elements increases. Stresses are evaluated in the element nodes and gauss points as seen in Table 4.6.

The results of displacements and stresses for the selected points given in Figure 4.13 are drawn in Figure 4.15 and Figure 4.16, respectively.

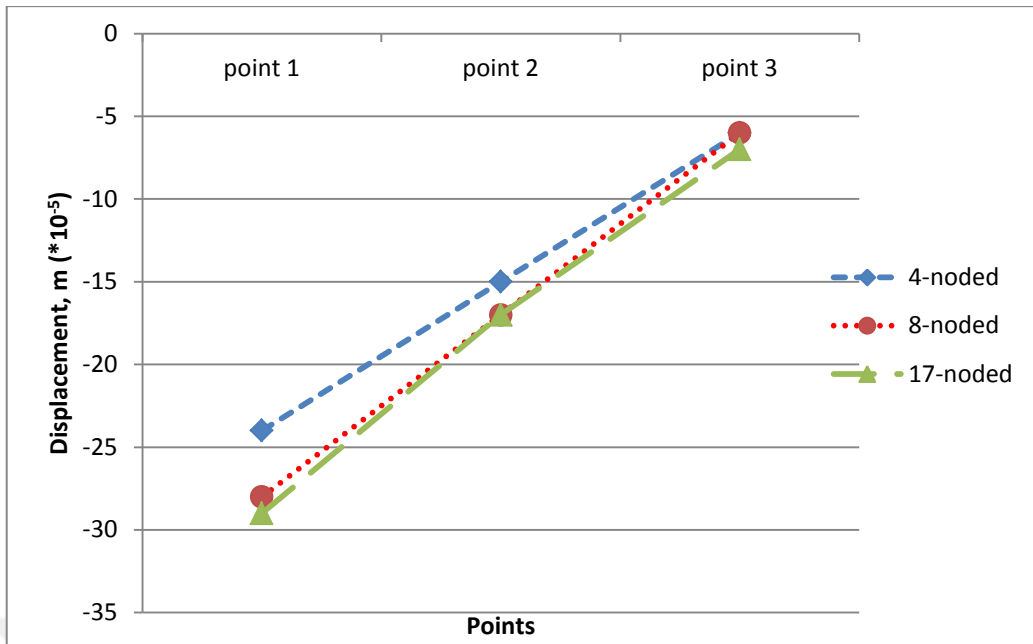


Figure 4.15 Displacement results for the retaining wall with FGM

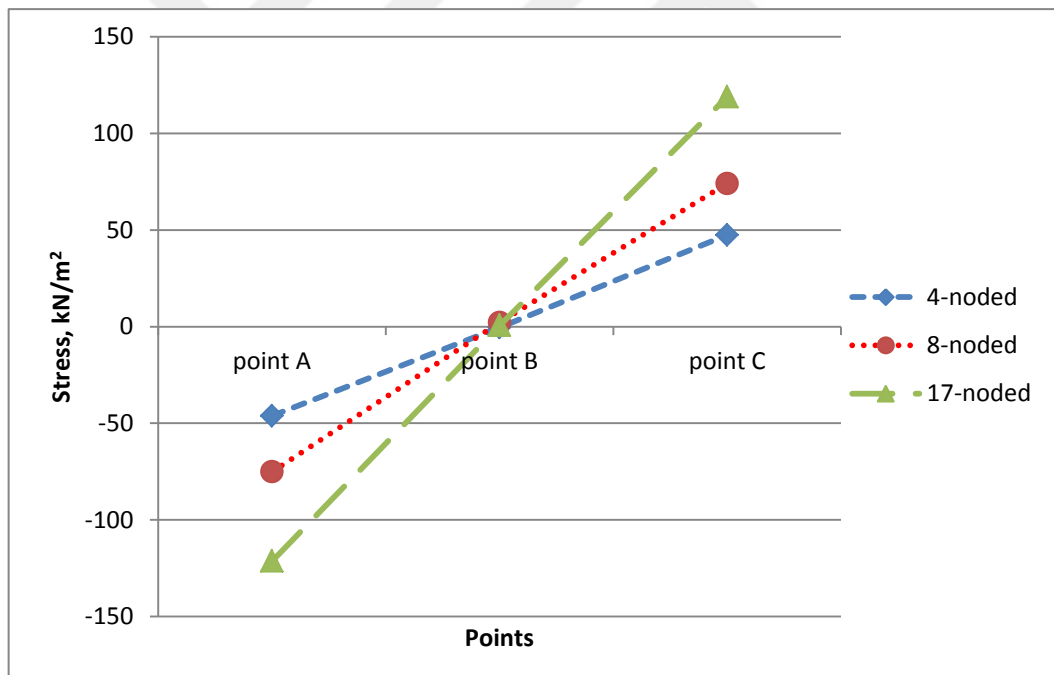


Figure 4.16 Stress results in horizontal direction for the retaining wall with FGM.

As seen in Figure 4.15 displacement results of the elements are so near. However, as seen in Figure 4.16 stress results keep developing when nodes within quadrilateral elements increase. It is expected that the stresses developed because these points are forced to tension stress in point C and compression stress in point A.

4.3.2 An Embedded Water Tank with FGM

An embedded water tank represents an axially symmetric 3D system, reduced to 2D system. It is considered as a plane stress problem. The tank is made from concrete which modulus of elasticity, E , is 3.0×10^6 kN/m², and Poisson ratio, ν , is 0.2. The functionally graded soil surrounds the tank, where there is a mixture of sand (Modulus of elasticity, E , is 2.0×10^4 kN/m², and Poisson ratio, ν , is 0.2) and clay (Modulus of elasticity, E , is 4590 kN/m², and Poisson ratio, ν , is 0.35). Material index (n) which indicates the material variation profile along the thickness of FGM, is taken as 5. The water density, γ_w is 1 kN/m³. Structure dimensions are demonstrated in Figure 4.17.

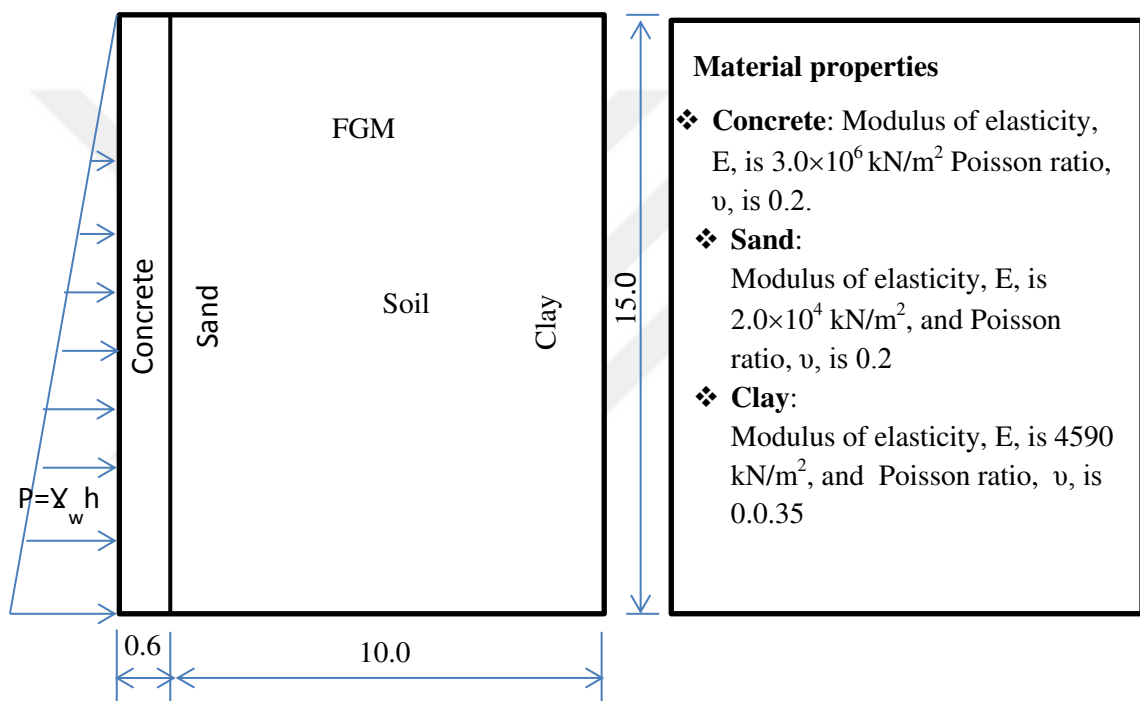


Figure 4.17 Structure dimensions for an embedded water tank

Displacement results are given for point 1, 2,3 and 4 which are seen in Figure (4.18).

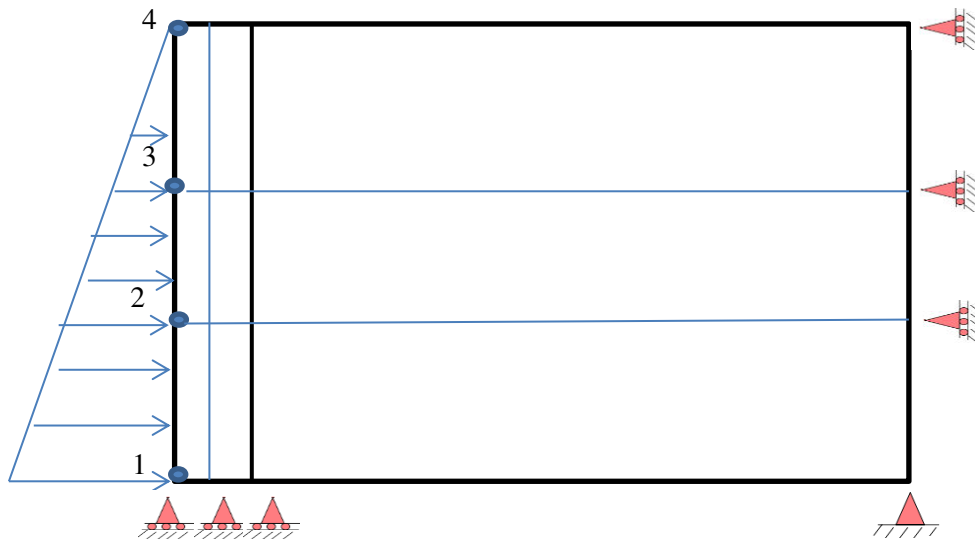


Figure 4.18 Mesh structure of an embedded water tank

When using 4-noded element, the deformed shape is shown in Figure 4.19.

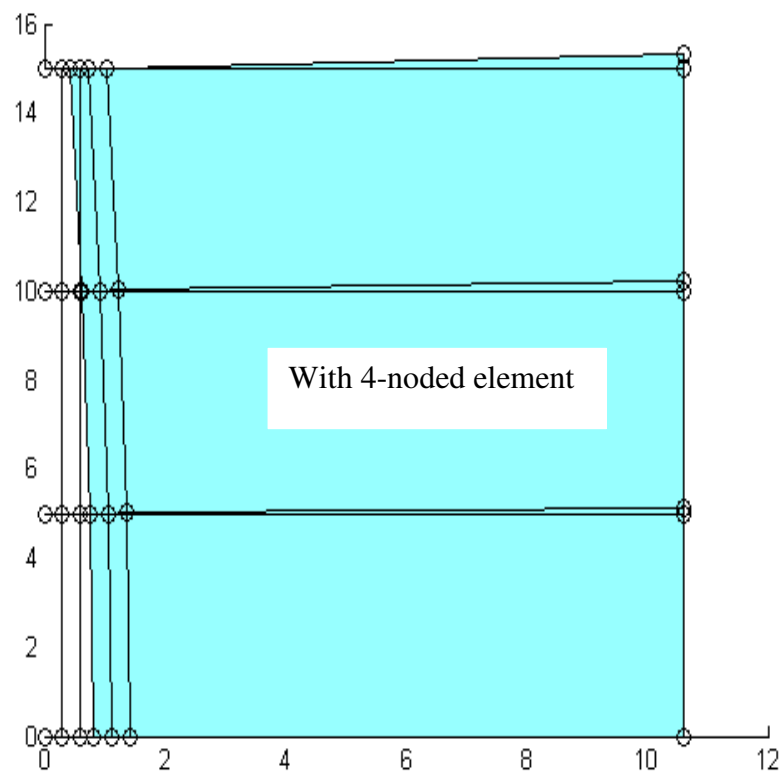


Figure 4.19 The deformed shapes for the embedded water tank

The results of selected points are shown in Figure 4.18 are given in the Table 4.7.

Table 4.7 Displacement and stress results of the embedded water tank.

Element type	Number of gauss points	Displacement in horizontal direction, m ($\times 10^{-5}$)				Stress in horizontal direction, kN/m ²							
		1	2	3	4	1		2		3		4	
						Element nodes	Gauss points	Element nodes	Gauss points	Element nodes	Gauss points	Element nodes	Gauss points
4-noded	2	0.17	0.16	0.13	0.09	-231.59	-194.06	-188.61	-159.85	-108.24	-95.72	-61.01	-60.10
8-noded	3	0.23	0.20	0.13	0.05	-140.86	-140.96	-127.25	-124.66	-80.19	-80.98	-37.47	-47.76
17-noded	5	0.24	0.20	0.13	0.05	-159.79	-155.83	-128.96	-124.18	-132.00	-68.42	-1.42	-64.43

As seen in Table 4.7, the range of difference is 4.0 % between 8-, and 17- noded elements. Moreover, 4-noded element gives less result of displacement than the results of the other elements.

Stresses decreases from point 1 to point 4 as expected. Moreover, results of stresses almost decrease when the number of node within quadrilateral elements increases. Stresses are evaluated in the element nodes and gauss points as seen in Table 4.7.

The results of displacements and stresses for the selected points given in Figure 4.18 are drawn in Figure 4.20 and Figure 4.21, respectively.

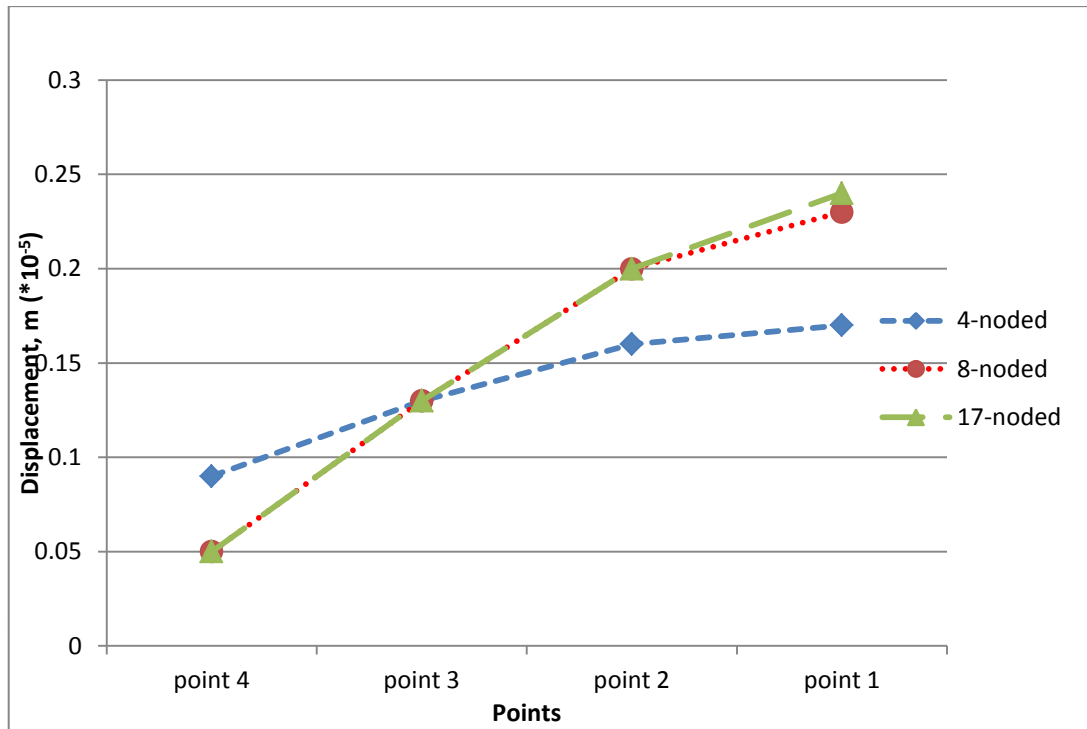


Figure 4.20 Displacement results for the embedded water tank.

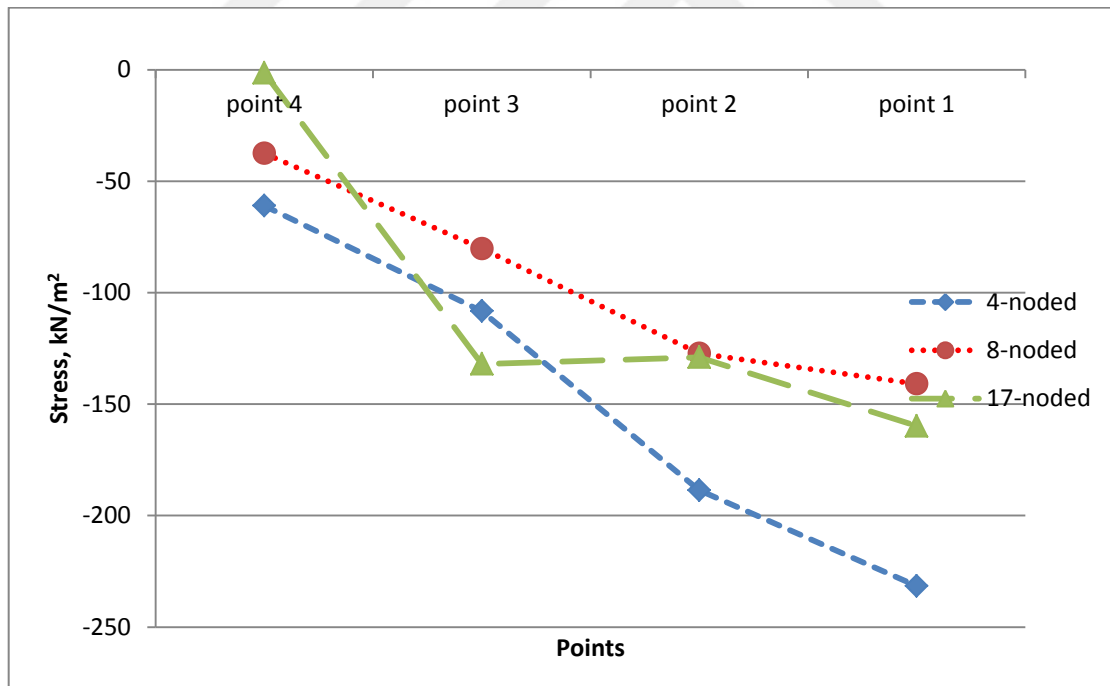


Figure 4.21 Stress results in horizontal direction for the embedded water tank

As seen in Figure 4.20 displacement results of the elements are so near. However, as seen in Figure 4.21 stress results keep developing when nodes within quadrilateral elements increase.

CHAPTER 5

CONCLUSION

This study was motivated to develop a finite element code, with high accuracy, by using higher order elements. The developed FE-code had the ability of dealing with Functionally Graded Materials (FGM).

The FE-code consisted of a 4-, 8-, and 17-noded quadrilateral finite elements. In order to get a more complete view, numerical results were achieved and verified for different problems to show accuracy and reliability of the FE-code. The given results in literature as exact and numerical values of some problems and results obtained within ABAQUS were used to compare results.

The following points are highlighted:

- The developed FE-code with 4-, 8-, and 17-noded elements satisfies patch tests.
- The FE-code gave acceptable displacement and stress results when they are compared with results of ABAQUS.
- The FE-code was applied to different field problems such as retaining wall, a deformed steel beam, and water embedded tank problems.
- Displacement and stress results are getting converged while the number of nodes within quadrilateral elements increases in the FE-code.
- The FE-code was successfully implemented on Functionally Graded Material problems. Moreover converged displacement and stress results were obtained.

- Future study may insert an ability to deal with the Functionally Graded Material (FGM) gradients of which are in 2D or 3D.
- Different type of interpolation function can be adapted to the FE-code to increase accuracy of the results.



REFERENCES

- [1] Ergatoudis, I. et al (1968). Curved Isoparametric, "Quadrilateral" Elements For Finite Element Analysis, *Int. J. Solids Structures*. 4:31-42.
- [2] William, F. (2015). How High a Degree is High Enough for High Order Finite Elements, *Procedia Computer Science*, 246-255.
- [3] Logan, L. (2007). *A First Course in the Finite Element Method*, 4th, Chris Carson, Canada, 475.
- [4] Tejaswini, N. (2015). "Functionally Graded Material: Overview", *International Journal of Advances in Engineering Science and Technology*, IJAEST, 4(3): 183-188.
- [5] Bharti, I. (2013). "Novel Applications of Functionally Graded Nano", *Optoelectronic and Thermoelectric Materials International Journal of Materials, Mechanics and Manufacturing*, 1(3): 221.
- [6] Koizumi, M. (1997). *FGM activities in Japan*, Elsevier Science Limited, *Composites Part B* 28B 1-4.
- [7] Miyamoto, Y. (1999). *Functionally Graded Materials: design, processing and applications*. Kluwer Academic Publishers.
- [8] Xiao, H. and Qi Yue, Z. (2012). Stresses and Displacements in Functionally Graded Materials of Semi-Infinite Extent Induced by Rectangular Loadings, *Materials*, 5: 210-226.
- [9] B.L. Shao, R.Q. Xu, *Axisymmetrical Analysis of Functionally Graded Circular Piezoelectric Plate by Graded Element Using MATLAB*, <https://www.researchgate.net/publication/253610047>, 15/2/2017.
- [10] Anandrao, K. (2012). "Free Vibration Analysis of Functionally Graded Beams", *Defence Science Journal*, 62(3):139-146.
- [11] Makwana, B. (2014). "Stress Analysis of Functionally Graded Material Plate with Cut-out", *International Journal of Advanced Mechanical Engineering*, 4(5):495-500.

- [12] Bhandari, M. Dr. Purohit, K. (2014). "Analysis of Functionally Graded Material Plate under Transverse Load for Various Boundary Conditions", Journal of Mechanical and Civil Engineering, 46-55.
- [13] Natarajan, S.et al., (2014). Analysis of Functionally Graded Material Plates Using Triangular Elements with Cell-Based Smoothed Discrete Shear Gap Method, Mathematical Problems in Engineering, Article ID 247932, 13.
- [14] Nguyen, T.N (2017). Iso-geometric analysis of functionally graded plates based on a new polynomial displacement field, Mechanics of Structures and Materials: Advancements and Challenges – Hao & Zhang (Eds) © 2017 Taylor & Francis Group, London, ISBN 978-1-138-02993-4, 1:606.
- [15] Oñate, E. (2009). Structural Analysis with the Finite Element Method Linear Statics. Basis and Solids, Springer, Spain, 1: 3-6.
- [16] Bekiroğlu S. (2006). "Development and verification of HP-FEM elastostatic plane problems", Seventh International Congress on Advances in Civil Engineering, Yildiz Technical University, Istanbul, Turkey.
- [17] Introduction to FEM, <http://www.colorado.edu/engineering/CAS/courses.d/IFEM.d/IFEM.Ch16.d/IFEM.Ch16.Slides.d/IFEM.Ch16.Slides.pdf>, 23/2/2017.
- [18] Khennane, A. (2013). Introduction to Finite Element Analysis Using MATLAB® and Abaqus, Taylor & Francis Group, 370-377.
- [19] Özdemir, Y. I. (2007). Shear locking-free analysis of thick plates using Mindlin's theory, Structural Engineering and Mechanics, 27(3):311-331.
- [20] Bekiroğlu,S., (2010). P-yöntemine dayali üç boyutlu sonlu elemanlar ile yapıları elastostatik ve elastodinamik analizi, PHD Thesis, Karadeniz University Graduated School, Trabzon.
- [21] Nakamura. T., (2000). determination of properties of graded materials by inverse analysis and instrumented indentation, Acta-Metallurgica Inc., 48(17): 4293–4306.
- [22] Smith, I. M., Griffiths, D. V. (2004). Programming the Finite Programming the Finite, 4th, John Wiley & Sons Ltd, England: 55.
- [23] Zienkiewicz, O. C (2000). The finite element method, 1:386, 4th, McGraw-HILL Company, Swansea.

CURRICULUM VITAE

PERSONAL INFORMATION

Name Surname : HANAN ALIMAM
Date of birth and place : 1972 IRAQ-BAGHDAD
Foreign Languages : ENGLISH
E-mail : hanan_alemam@yahoo.com

EDUCATION

Degree	Department	University	Date of Graduation
Master			
Undergraduate	Civil engineer	Almustansiriya university	1994
High School	Scientific Part	Alakedaa	1989

WORK EXPERIENCE

Year	Corporation/Institute	Enrollment
2005-2014	Ministry of Education/ Educational buildings	25-9-2014
1996-2001	Ministry of Industry	4-6-1996

Conference Papers

1. Alimam H., Bekirođlu S., 2017, Finite Element Modelling Of A Retaining Wall With Functionally Graded Material, International Conference On Advances In Science And Arts, ICAS, 29-31 March 2017, Istanbul, Turkey. ISBN 978-605-9546-03-4, p 278.

